AD-A138 230 A MINIMUM RANGE CRITERION FOR RCS (RADAR CROSS-SECTION) 1/2
MEASUREMENTS OF A..(U) AIR FORCE INST OF TECH
WRIGHT-PATTERSON AFB OH SCHOOL OF ENGI.. B M WELSH
UNCLASSIFIED DEC 83 AFIT/GE/EE/83D-71 F/G 17/9 NL

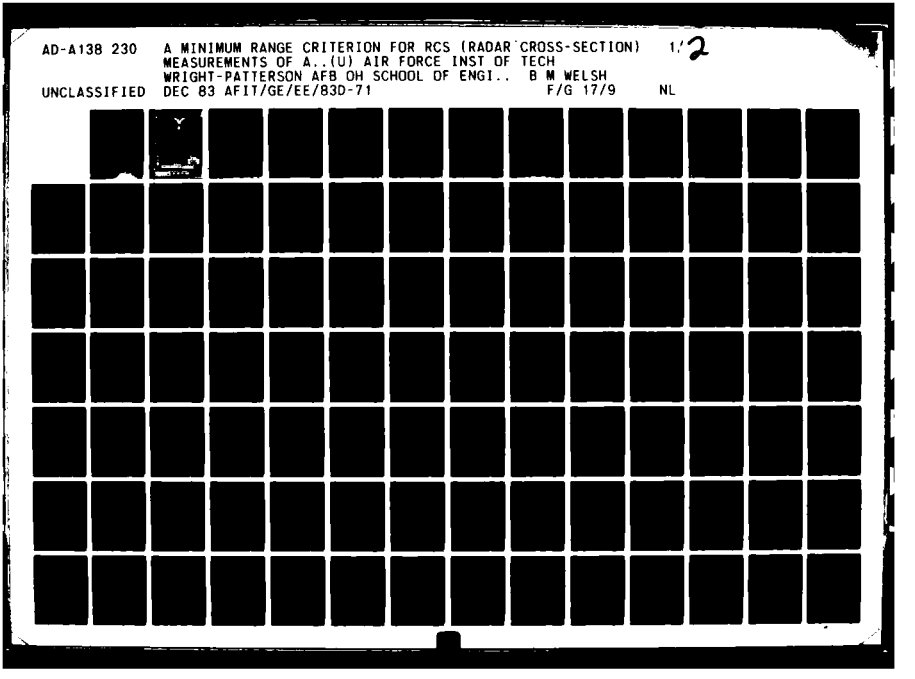

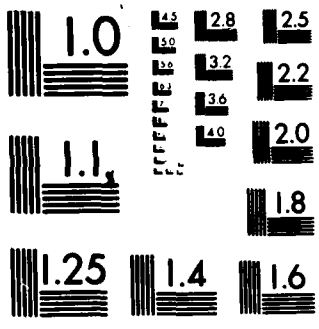

A MINIMUM RANGE CRITERION FOR RCS MEASUREMENTS OF A TARGET DOMINATED BY POINT SCATTERERS

THESIS

AFIT/GE/EE/83D-71

Byron M. Welsh
2nd Lt USAF

AFIT/GE/EE/83D-71

A MINIMUM RANGE CRITERION FOR RCS MEASUREMENTS OF A TARGET DOMINATED BY POINT SCATTERERS

THESIS

AFIT/GE/EE/83D-71 Byron M. Welsh
2nd Lt USAF

AFIT/GE/EE/83D-71

A MINIMUM RANGE CRITERION FOR RCS MEASUREMENTS OF A TARGET DOMINATED BY POINT SCATTERERS

THESIS

Presented to the Faculty of the School of Engineering
of the Air Force Institute of Technology
Air University
in Partial Fulfillment of the
Requirements for the Degree of
Master of Science

by
Byron M. Welsh
2nd Lt USAF
Graduate Electrical Engineering
December 1983

Preface

I thank Captain T. Johnson for his time, support and guidance given to me during this thesis work. I also thank Mr. Bill Kent for his time, support and guidance as my thesis sponsor. I especially thank my wife, Nancyanne, for her patience, love and constant encouragement given to me during this past year.

Byron M. Welsh

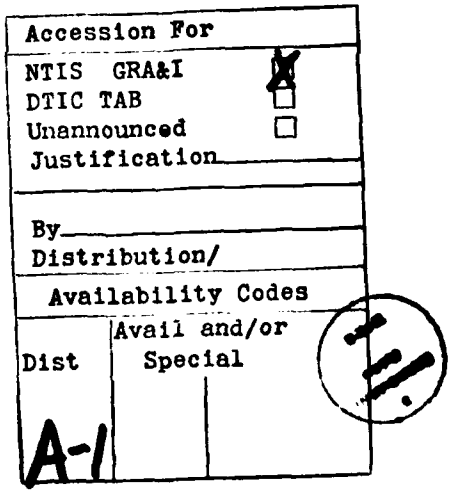

Contents

List of Figures

Abstract

This thesis develops a minimum range criterion for radar cross section measurements by neglecting the phase of the incident field at the target and considering only the amplitude distribution. In contrast to the traditional minimum range criterion, developed for a flat target characterized by specular reflection, the target examined in this thesis is characterized by a number of independent point scatterers located on the target surface. Instead of enforcing point by point accuracy, accuracy of the average target RCS is required, averaging over a number of measurements. The location of the point scatterers on the target are described probabilistically; the expected average measured RCS versus target range is calculated, and compared to results of a Monte-Carlo simulation. The traditional minimum range criterion is compared to the new minimum range criterion. The traditional minimum range criterion, based on phase uniformity across the target, requires minimum measurement ranges that are much larger than those ranges dictated by the new minimum range criterion for targets dominated by point scattering.

A MINIMUM RANGE CRITERION FOR RCS MEASUREMENTS OF A TARGET DOMINATED BY POINT SCATTERERS

I. Introduction

Background

The radar cross-section (RCS) of a target is simply a measure of the electromagnetic energy scattered from the target normalized to the electromagnetic energy incident on the target. The RCS of a target can be determined either experimentally or theoretically. Theoretical calculation of the RCS of a complex target (such as an aircraft) is complicated and time consuming, and it is for this reason that RCS measurements are important. RCS measurements are also needed to verify the theoretical solutions for certain simple targets. Ultimately, RCS measurements simulate the interaction of the target with a radar in a "real" engagement.

Many factors affect the accuracy of RCS measurements. The distance (range) the target is separated from the source is one of these factors. The definition of RCS assumes that the incident electromagnetic wave at the target is a plane wave and that the radar receiver is in the "far field" of the target. The electromagnetic wave emitted from an antenna is a spherical wave, and if the target is in the far field of the antenna, the

spherical wave approximates a plane wave to the extent necessary to make a useful measurement. Although theoretically the spherical wave becomes a plane wave at an infinite distance from the antenna, the typical criterion used for being in the "far field" is that the incident field, at the target, must not vary in phase in the transverse direction (perpendicular to direction of propagation) more than $\pi/8$ radians over the extent of the target. The amplitude variation in the radial (direction of propagation) and transverse direction must not be more than 1 db over the extent of the target (Ref 7:921).

The minimum RCS measurement range based on the above limits is

$$R_m = \frac{2L^2}{\lambda}$$

where R_m is the minimum range, L is the maximum dimension of the target and λ is the wavelength of the incident wave. This range criterion results in a maximum deviation of the measured RCS compared to the true far field RCS of 1 db. Note that this range criterion is based on a flat target dominated by specular reflection (Ref 7:921).

A simple example using the above range criterion shows some problems associated with it. For a target that is 10 meters long and being measured at a frequency of 10 GHz, the minimum range is 6.66 km. A 6.66 km range is impractical to

build because of the large physical measurement area and sophisticated equipment required. The largest range at the RAT SCAT cross section facility located near Holloman AFB, New Mexico, is only 2.3 km long. Measurements are much easier to make for short ranges since less space is needed and the demands of the measurement equipment are less rigorous.

The applicability of the range criterion ($2L^2/\lambda$), developed for the field scattered from a flat target, is unknown for a target dominated by point scatterers and of such a size that only averages or percentile data are useful. A point scattering target is characterized by elimination of all specular points and scattering only from independent point scatterers located on the target surface. The target of interest today is often a complex aircraft that can be characterized as a distribution of point scatterers.

Problem

Develop a minimum range criterion for acceptable RCS measurements for the general target dominated by point scatterers.

Scope

This thesis will solve the problem of determining the RCS of the general target dominated by point scatterers at various ranges. Specific targets, such as an aircraft, will not be considered. The point scattering target will be modeled

statistically and only a theoretical approach will be taken in solving for the RCS. No actual RCS measurements will be made.

Assumptions

1. The field scattered from the target (statistical model) is assumed to be accurately described by Petr Beckmann in his journal article, "Statistical Distribution of the Amplitude and Phase of a Multiply Scattered Field" (Ref 1: 231-240).

2. The detector used to measure the scattered field strength from the target will not affect the scattered field.

3. Scattering from background clutter will be nonexistent and only the target scattering will be present at the detector.

4. The modeled target will consist of many point scatterers of negligibly small dimensions and the fields scattered from each of the point scatters will be independent of other scattered fields.

Approach

A general ground bounce RCS measurement range is modeled using a parabolic reflector dish as the measurement antenna. The field pattern set up by the antenna is found using aperture integration. The ground bounce characteristic of the measurement range is modeled by removing the ground plane and placing the image of the measurement antenna below the ground level.

Once the RCS measurement range has been modeled, the target is introduced. The target is modeled as a statistical distribution of point scatterers along a straight length, L. Uniform, stepped uniform and truncated Gaussian spatial distributions of the point scatterers along L are used.

Analytical and Monte-Carlo approaches are used to calculate the mean of the measured RCS. The analytical approach involves approximating the complicated antenna pattern, derived in the RCS measurement model, by a simple function. Once an approximation is made, the mean of the measured RCS is calculated.

The Monte-Carlo approach involves using the derived antenna pattern and randomly located point scatterers to numerically simulate the process of measuring and finding the mean of the RCS. This approach is used to verify the results of the analytical approach.

At this point the target range is varied and the effect on the average measured RCS is examined using the analytical and Monte-Carlo approaches. The results from the two approaches show the RCS variation as the target range is varied. This RCS variation versus range data shows how much RCS error (compared to the true measured RCS at very large ranges) can be expected for various range reductions. A minimum range criterion is obtained from the RCS variation versus range data.

Development

The structure of this thesis is outlined below:

Chapter II reviews the traditional approach of developing a minimum range criterion for RCS measurements. This chapter discusses the assumptions, criteria, and reasoning used in developing the minimum range criterion for the target dominated by specular scattering.

Chapter III reviews a different (existing but not canonical) approach of developing a minimum range criterion. This chapter reviews an article by Lee Hendrick (Ref 4:5-19). In this article, Hendrick considers the target dominated by diffracting centers. Hendrick models the target deterministically by using three point scatterers placed in a triangular arrangement. Hendrick develops a minimum range criterion based on the modeled target.

Chapters IV and V starts the new development of a minimum range criterion for the target dominated by point scattering. These chapters detail the development of the RCS measurement range model and the statistical target models. The RCS measurement range model simulates the antenna pattern that would exist at a typical RCS measurement range such as RAT SCAT. The target models simulate targets dominated by point scattering and are described statistically, unlike the target models used by Hendrick in Chapter III.

Chapter VI reviews the general statistics of multiply scattered fields. These general statistics are then applied to

the specific fields scattered from the modeled targets.

Chapters VII and VIII introduce the methods used to develop the minimum range criterion and the results of these methods. The two methods include an analytical approach and a Monte-Carlo simulation to calculate the average measured RCS.

Chapter IX develops the vertical 3 db beamwidth of the antenna pattern derived in Chapter IV. The vertical 3 db beamwidth is needed to apply the minimum range criterion, developed in Chapter VIII, to the vertically oriented target.

Chapter X gives an overview of the approach taken to develop the new minimum range criterion and illustrates use of the criterion by showing some examples.

II. Traditional Approach

Introduction

The traditional range criterion for RCS measurements is presented by R. G. Kouyoumjian and L. Peters, Jr. (Ref 7:920-928). This chapter reviews the derivations and conclusions made by Kouyoumjian and Peters. The chapter is organized in the following manner: First, the approximation of a spherical wave as a plane wave is discussed, and the impact of the inaccuracies inherent in this approximation (both phase and magnitude) is assessed. A simple example, measurements of the RCS of a disk, illustrates these points. Next, the phase taper seen by the target, produced by approximating the antenna as a point source, is calculated. The amplitude variation along a radial path from the source is briefly discussed. Finally, the amplitude and phase taper of the incident field, produced by a uniform square aperture (assumed as the source), is analyzed in terms of both antenna dimension and target dimension.

Background

The RCS of a target is defined by

$$\sigma = \lim_{R \to \infty} 4\pi R^2 \frac{\left|E_A^s\right|^2}{\left|E_A^i\right|^2}$$

where R is the distance between the target and the radar antenna. $\bar{E}^s_{\hat{x}}$ and $\bar{E}^i_{\hat{x}}$ are the scattered and incident electric fields respectively, both linearly polarized in the $\hat{x}$ direction. The incident electric field must be a plane wave in the vicinity of the target to satisfy the RCS definition. If the incident electric field forms a spherical wave front and the target is not in the far zone of the source, RCS measurement errors will result. If the target is in the far zone of the source antenna, the spherical wave becomes a plane wave. Theoretically, the "far zone" is located at infinity and for ranges less than infinity the spherical wave only approximates a plane wave. The amount of transverse phase and amplitude variation of the incident field over the extent of the target is used to gauge how well the spherical wave approximates a plane wave. The "extent of the target" refers to the maximum dimension of the target in the transverse direction (perpendicular to propagation).

It has been found through measurements and experience that RCS measurements can be made with acceptable accuracy when the phase variation of the incident field does not exceed $\pi/8$ radians and the amplitude variation does not exceed 1 db over the extent of the target. The RCS measurement error produced by the above variations in phase and amplitude will generally be less than 1 db. It has also been found that the phase variation can exceed π radians for large targets characterized by a number of scattering centers, and in this case the

amplitude variation must be less than 3 db. For accurate RCS measurements of a flat target, the phase variation must not exceed $\pi/16$ radians and the amplitude variation must not exceed 0.2 db. The traditional minimum range criterion is developed to satisfy these phase and amplitude variation criteria.

RCS of a Flat Circular Plate

To illustrate the effects of phase and amplitude variation on RCS measurements, the RCS of a large circular plate is calculated by the use of physical optics. The RCS calculations are made for maximum phase variations of $\emptyset_m = 0$, $\pi/8$ and $\pi/4$ radians over the extent of the target. As seen in Figure II-1, the RCS of the circular plate can be measured with acceptable accuracy for a phase variation as large as $\pi/8$ radians. Values of $\emptyset_m$ greater than $\pi/8$ radians lead to large errors in the RCS measurements. The RCS nulls are the most affected by phase variation, and even at $\emptyset_m = \pi/8$ radians, the error in the nulls is quite significant. In many cases, the average RCS values are of prime importance, so the errors in the null depths are not a significant problem (Ref 7:923).

In the above discussion, the amplitude variation was assumed to be zero and the phase distribution varied from zero to $\pi/4$ radians. Now assume a zero phase variation over the

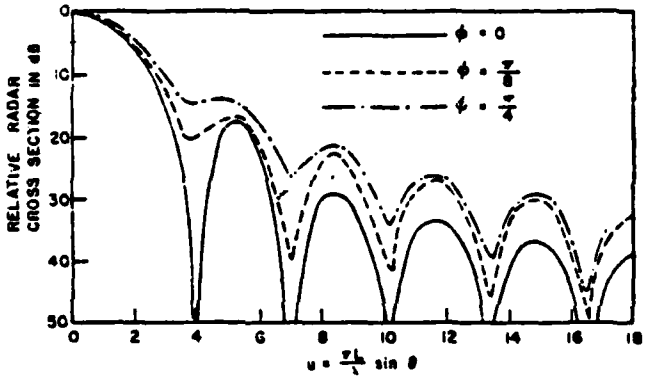

Fig. II-1. Radar Cross-Section of a Circular Plate with a Quadratic Phase Error

target and examine the effects of an amplitude variation. From antenna theory it is known that a tapered amplitude distribution on an antenna will cause a broadening of the main lobe and a decrease in the side lobe levels, compared to a uniform amplitude distribution. This is also the case for a tapered amplitude distribution over the target. For a 1 db amplitude variation of the incident field, an error of 2.5 db for the first side lobe of the RCS pattern will be measured, which is the upper limit of error that can be tolerated. The main lobe of the RCS pattern is not affected by the amplitude variation to such a large degree as the side lobes.

The Minimum Range Criterion for a Point Source Antenna

The gauge of how well a spherical wave approximates a plane wave can be expressed mathematically as

$$\frac{E^i(L/2)}{E^i(0)} = A_m e^{j\phi_m} \qquad \text{(II-1)}$$

where L is the maximum dimension of the target and $E^i(x)$ is the amplitude and phase of the incident electric field at the target (see Figure II-2). The amplitude and phase variation

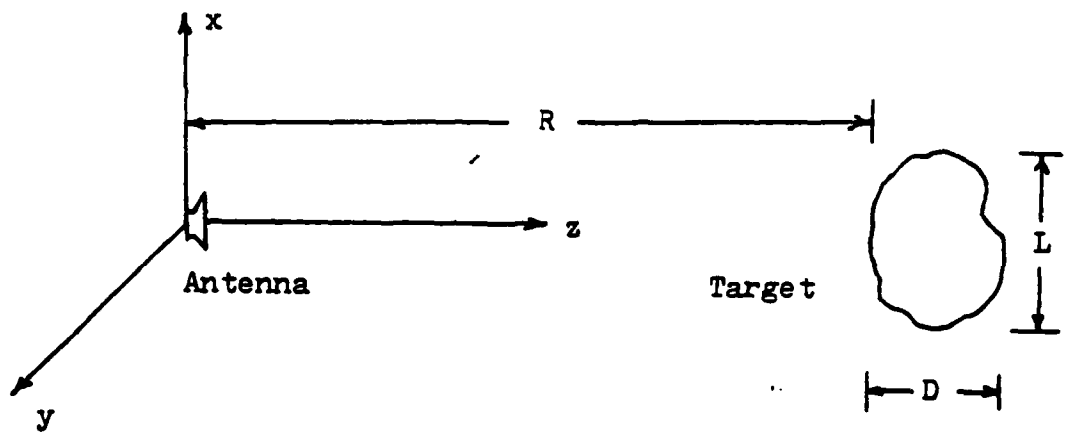

Fig. II-2 Antenna Range and Target Configuration

over the extent of the target are designated by A_m and ϕ_m. If the incident field is a plane wave then $A_m = 1$ and $\phi_m = 0$. The minimum range criterion limited by the maximum phase variation will be developed first. By considering the antenna a point source and the target a flat plate, the phase variation over the target can be calculated (see Figure II-3). The maximum phase deviation from the center of the target is

$$\phi_m = \frac{2\pi}{\lambda}(r - R_m) = \frac{2\pi}{\lambda}\left[\sqrt{R_m^2 - (L/2)^2} - R_m\right]$$

where ϕ_m and R_m are the maximum phase variation and minimum range criterion respectively. Using the binomial expansion

$$\phi_m = \frac{2\pi}{\lambda}\left[\frac{L^2}{8R_m} - \frac{L^4}{128R_m^3} + \cdots\right]$$

For $R_m >> L$

$$\phi_m \cong \frac{2\pi}{\lambda}\left[\frac{L^2}{8R_m}\right]$$

The minimum range is

$$R_m \cong \frac{2\pi}{\lambda}\left[\frac{L^2}{8\phi_m}\right]$$

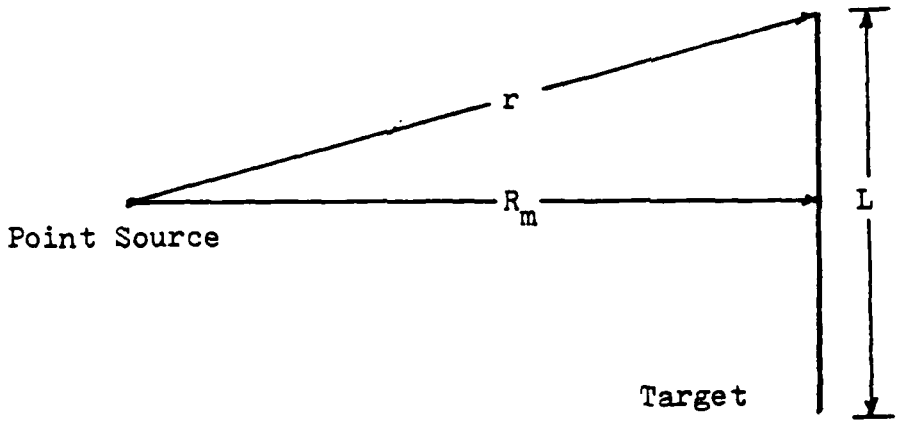

Fig. II-3. Point Source and Flat Target Configuration

and forcing $p = \pi/(4\phi_m)$

$$R_m = \frac{pL^2}{\lambda} \qquad \text{(II-2)}$$

Eq (II-2) is the traditional minimum range criterion for the point source antenna illuminating a flat target.

The minimum range criterion limited by the maximum amplitude variation will now be developed. The amplitude variation in the axial and transverse directions must be considered. If the maximum allowable amplitude variation in the transverse direction is 1 db, then the maximum amplitude variation in the axial direction should also be fixed at 1 db. Assuming the target is far enough away from the antenna for the magnitude of the electric field to have a $1/R_m$ dependence then the minimum range criterion can be expressed as

$$20\text{Log}\left(\frac{1}{R_m}\right) - 20\text{Log}\left(\frac{1}{R_m+D}\right) \leq 20\text{Log}(A_m) \qquad \text{(II-3)}$$

Eq (II-3) only takes the axial amplitude variation into account. D is the maximum longitudinal dimension of the target. For a maximum axial amplitude variation of 1 db, R_m must be greater than 8D. Usually the minimum range is limited not by the axial amplitude variation, but by the transverse amplitude variation which is determined mostly by the antenna pattern factor.

The Minimum Range Criterion for a Square Aperture Antenna

The minimum range will now be evaluated for a square aperture antenna with a side of length ℓ and a uniform field distribution over the aperture. The target will have a transverse dimension of L and will be a distance R_m from the antenna. The simplifications assumed for the aperture antenna will not make the problem unrealistic, but will give results that will be generally applicable for aperture antennas of comparable size.

The minimum range will be determined with A_m and ϕ_m of Eq (II-1) fixed and ℓ/L a variable. The field produced by a square aperture lying in the XY plane with a uniform aperture field distribution is given by

$$E_x = \frac{jE^a}{2} e^{-j\beta z}\left[E\left(\frac{\ell+2x}{\sqrt{2\lambda z}}\right) + E\left(\frac{\ell-2x}{\sqrt{2\lambda z}}\right)\right]$$

$$\cdot \left[E\left(\frac{\ell+2y}{\sqrt{2\lambda z}}\right) + E\left(\frac{\ell-2y}{\sqrt{2\lambda z}}\right)\right] \qquad \text{(II-4)}$$

where

$$E(\tau) = \int_0^{\tau} \exp(-j\,\frac{\pi}{2}\,\alpha^2)\,d\alpha$$

is a Fresnel integral (Ref 6:132). The expression for $A_m e^{-j\phi_m}$ can now be written

$$A_m e^{-j\phi_m} = \frac{E\left(\frac{\ell+L}{\sqrt{2\lambda R_m}}\right) + E\left(\frac{\ell-L}{\sqrt{2\lambda R_m}}\right)}{2E\left(\frac{\ell}{\sqrt{2\lambda R_m}}\right)} \qquad \text{(II-5)}$$

After considerable manipulation of Eq (II-5) (Ref 7:924-925), the resulting minimum range criterion is shown in Figure II-4. Figure II-4 is a graph of the normalized minimum range criterion versus ℓ/L for particular values of A_m and ϕ_m. From the graph it is seen how important it is to consider the dimension of the antenna when determining the minimum range. For the criteria of $\phi_m = \pi/8$ radians and $A_m = 1$ db it can be seen that the minimum range is phase limited between $\ell/L = 0$ and $\ell/L = 1$, and amplitude limited for $\ell/L > 1.0$.

Summary

In the traditional approach, the maximum allowable phase and amplitude variation of the incident field across the target is used to specify the minimum RCS measurement range. The traditional minimum range criterion is also based on a flat target with the broadside oriented toward the radar. Two

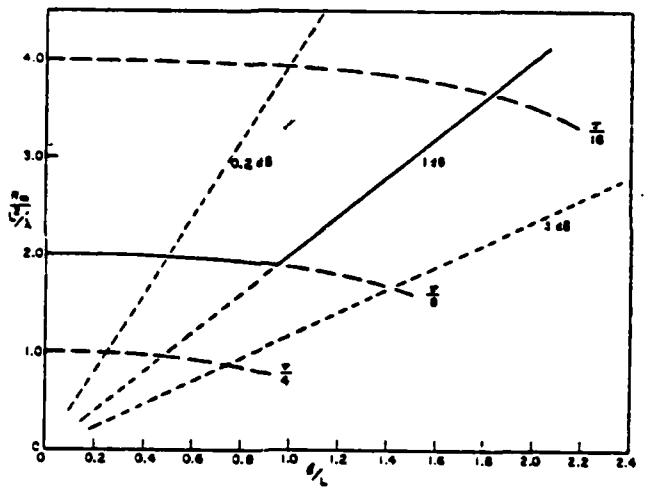

Fig. II-4. Normalized Minimum Range Criterion for a Square Aperture Antenna

minimum range criteria are derived. For the point source antenna, the minimum range criterion is stated as

$$R_m = \frac{\pi L^2}{4\phi_m \lambda} = \frac{DL^2}{\lambda} \qquad \text{(II-6)}$$

For the square aperture antenna, of comparable size to the target, the minimum range criterion is altered from Eq (II-6) as shown in Figure II-4.

III. Analytical Investigations of a Reduced RCS Range Criterion

Introduction

This section reviews a paper written by Lee R. Hendrick entitled "Analytical Investigation of Near-Zone/Far-Zone Criteria," (Ref 4:5-19). In it, the effects of antenna to target range reductions for a target modeled by a simple distribution of point scatterers are studied.

Background

In Chapter II the minimum range criterion was developed for a flat plate scatterer. The minimum range criterion was pL^2/λ, where L was the maximum dimension of the target, λ was the wavelength of the incident wave and p was proportional to the maximum phase variation across the target. As already stressed in Chapter I, reduction of the minimum range criterion is very desirable. Hendrick amplifies this need for a reduced range criterion and shows, as a result of his work, that: (1) the minimum range criterion is closely related to whether exact or average RCS data is wanted; (2) for most situations in which the required RCS data is average RCS data, the range can be <u>less</u> than L^2/λ; (3) as the target size increases, the minimum range factor p can generally be reduced; (4) the antenna beamwidth is very important.

As pointed out previously, the incident electric field at the target must approximate a plane wave. When the range is

less than the range criterion established in the previous chapter, the incident wave deviates considerably from a plane wave. Also the magnitude of the field may deviate from the far field 1/R dependence and the antenna pattern will depart from the true far field pattern. Generally for a large complex target, the above deviations may not cause serious errors in the RCS measurements if only average RCS data is required.

Point Scatterer Models and RCS Calculations

Hendrick calculated the RCS of a target modeled as a distribution of three point scatterers The scatterers have negligibly small dimensions and are arranged in a triangular arrangement. Five models are used with lengths of 3λ, $3\frac{1}{2}\lambda$, 10λ, $10\frac{1}{2}\lambda$, and 50λ (see Figure III-1).

For each model the RCS is calculated at different ranges varying from $2L^2/\lambda$ to $L^2/4\lambda$. The beamwidth of the antenna pattern is also varied for each model. A wide and a matched beamwidth is used. The wide beamwidth is characterized by an almost flat amplitude distribution over the target, while the matched beamwidth has a 3 db beamwidth equal to the maximum dimension of the target.

The total electric field scattered from the model is found by taking the field scattered from each point scatterer and forming a complex sum of each. The radar range equation is used to define the RCS of each scatterer and the square-root of the RCS is used to calculate the scattered electric fields.

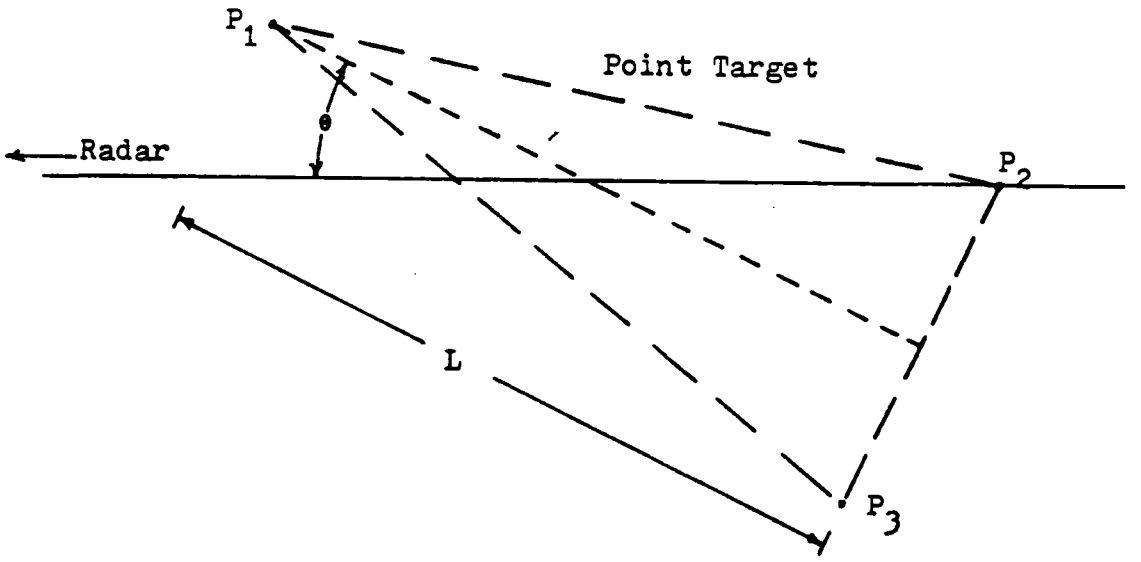

Fig. III-1. Basic Model Configuration

Results

Wide Beamwidth. The far field RCS is assumed to be the measurement taken at the longest range. The effects of reducing the range are examined.

For the short models (3λ and $3\frac{1}{2}\lambda$), the RCS calculations show degradation at a range of L^2/λ, and very bad degradation at a range of $L^2/2\lambda$. For the medium length model (10λ and $10\frac{1}{2}\lambda$), the angular spacing of the RCS maxima are not seriously affected down to a range of $\frac{1}{2}L^2/\lambda$. The deep nulls are not present but the average values of the RCS maxima are fairly well preserved. When the range is reduced from $2L^2/\lambda$ to $\frac{1}{2}L^2/\lambda$ for the 50λ target, the angular position of the nulls and maxima are displaced, but the values of the maxima and nulls are within 2 db of the far field values. Further reduction of the range for the 50λ target causes serious degradation of the nulls, but the average values of the maxima remain preserved down to $L^2/8\lambda$.

Matched Beam Results. For the short model (3λ), at reduced ranges there is loss of RCS null depth and at an aspect angle of 60 degrees the maxima are 5 db less than the wide beamwidth case. Since the angular density of the maxima is small for short targets, the RCS errors mentioned above, affect the average RCS more severely than for the longer targets.

For the medium length target (10λ), at reduced ranges, there is some RCS null depth loss, but the maxima remain at the

far field average for aspect angles less than 30 degrees. For aspect angles greater than 30 degrees there is a slight decrease in the magnitude of the RCS maxima. This decrease in magnitude is due to the amplitude taper over the target.

The RCS calculation for the long target using the matched beamwidth and a reduced range shows some loss of null depth. The maxima are nearly the same as the case for the wide beam.

From the above results, Hendrick suggested minimum range criteria for long, medium and short targets. These suggested criteria are shown in Table III-1. If a graph is made of minimum range versus maximum target dimension, a curve can be drawn through the three points. This graph can be used for rough estimation of the minimum range required. The graph is shown in Figure III-2.

Summary

Measurement ranges less than L^2/λ can be used with negligible RCS measurement error for targets consisting of only a few scattering centerers and of such a size that average RCS data is desired. For targets as long as 50λ, the range can be reduced to $L^2/4\lambda$. It is also noted that beamwidth considerations are very important. A narrow beamwidth will generally incur greater RCS errors than a reduced range.

Target Size, L/λ	Minimum Range, R
3	$4L^2/\lambda$
10	$L^2/2\lambda$
50	$L^2/4\lambda$

Table III-1. Minimum Range Criteria for Various Target Sizes

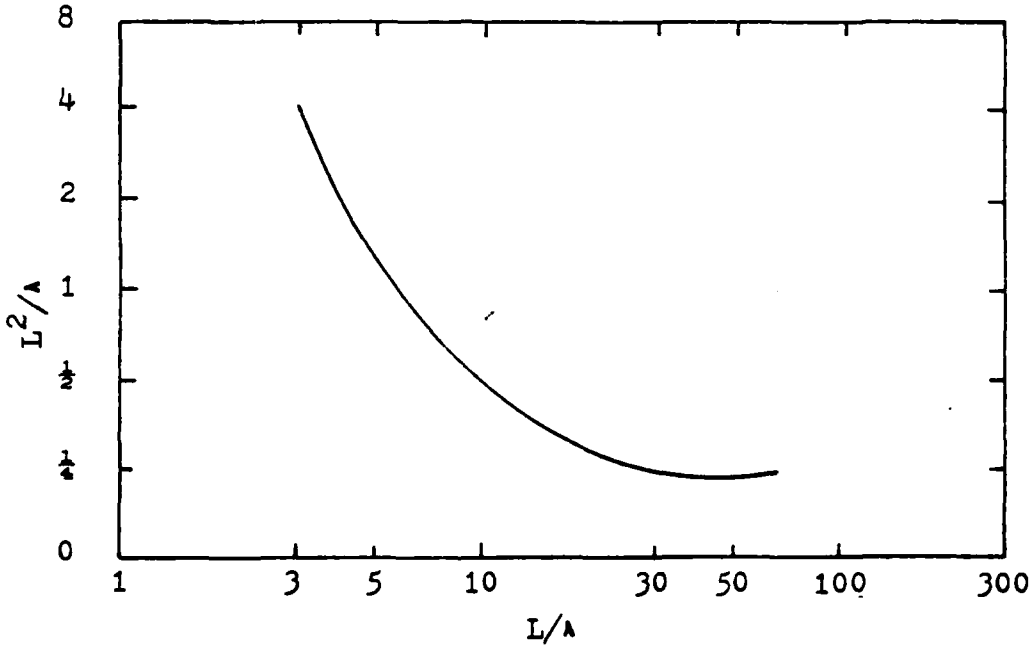

Fig. III-2. Hendrick's Minimum Range Criterion

IV. Model of Incident Field

Introduction

As outlined in the approach, the RCS of a target, consisting of a distribution of point scatterers, will be calculated at various ranges. The first step in this calculation is determining the incident electric field at the target. The amplitude of the incident field is needed. This chapter will review the criteria used to specify the antenna pattern and the approach used to calculate the incident field quantities.

Antenna and Range Characteristics

The incident electric field quantities at the target should closely resemble the fields measured at existing RCS measurement ranges, such as RAT SCAT. Some characteristics of the typical RCS measurement range are the use of a parabolic reflector antenna that can be tilted and a ground bounce range. By using a ground bounce range the target will see an array of two antennas in the vertical dimension due to the original antenna's image below the ground. The resulting antenna beam from the ground bounce range will be wider in the horizontal direction than in the vertical direction. This is desirable since targets are usually wide in the horizontal dimension and narrow in the vertical dimension.

When RCS measurements are made, generally a maximum of 1 db amplitude variation over the target aperture is tolerated, as discussed in Chapter II. Amplitude measurements of the incident field at the target are made to confirm the 1 db amplitude variation. Adjustments of the antenna parameters, such as height and tilt angle, are made to meet the 1 db amplitude variation criterion. A null in the antenna pattern at the base of the target support is also desirable. This null reduces the scattered return from the target support.

Calculations of the Antenna Field Pattern

Image theory is used to model the effect of the ground bounce range as seen in Figure IV-1. The measurement range model incorporates two antennas, one above the ground a height D, and one below the ground a depth D. The ground is effectively removed and the fields from both antennas can be added to get the total field.

The fields from the parabolic reflector antennas are calculated by using aperture integration. The aperture field distribution is assumed to be a parabolic taper on a pedestal. The aperture distribution for the parabolic reflector antenna is well approximated by this distribution (Ref 11:428). Aperture integration gives accurate results for observation points less than 30 degrees off the antenna axis and since RCS measurements are made with the antenna nearly pointing straight at the target, this limitation will not cause problems.

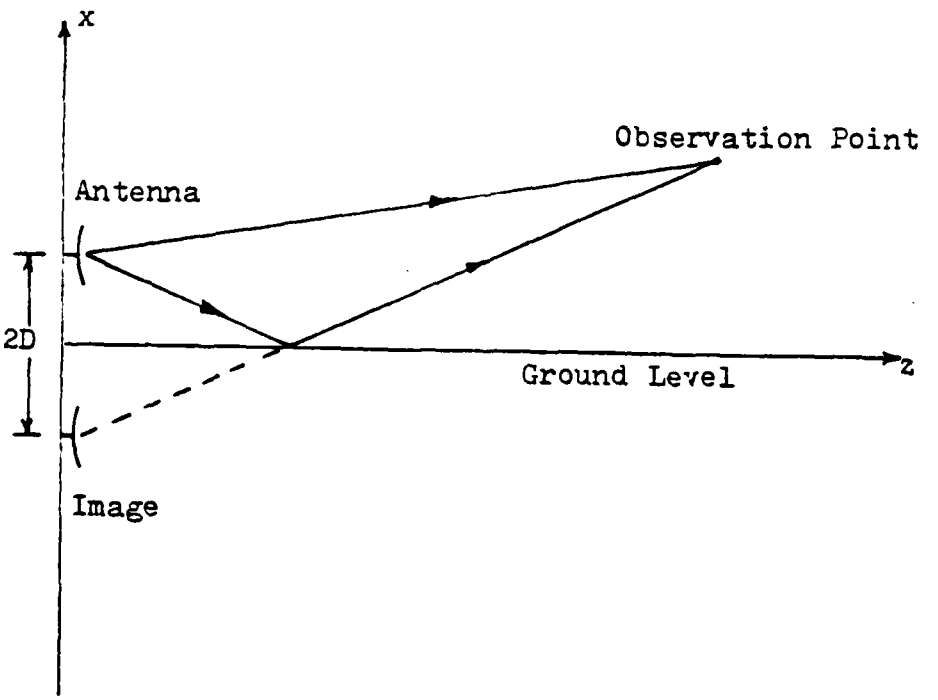

Fig. IV-1. Ground Bounce Range Configuration

Using the parabolic taper on a pedestal, the aperture field can be expressed as (Ref 11:420)

$$E_a(r') = C + (1-C)\left[1 - (r'/a)^2\right]$$

where

C is the pedestal height
a is the radius of the circular aperture
r' is the radial cylindrical coordinate located in the XY plane (see Figure IV-2)

The resulting fields from the aperture illumination are (see Appendix A for derivation)

$$E_\theta = \frac{j\omega(r)2\pi}{\sin\theta}\left[aCJ_1(\beta a \sin\theta) + \frac{2(1-C)J_2(\beta a \sin\theta)}{\beta \sin\theta}\right]\cos\phi \qquad \text{(IV-1)}$$

$$E_\phi = \frac{-j\omega(r)2\pi\cos\theta}{\sin\theta}\left[aCJ_1(\beta a \sin\theta) + \frac{2(1-C)J_2(\beta a \sin\theta)}{\beta \sin\theta}\right]\sin\phi \qquad \text{(IV-2)}$$

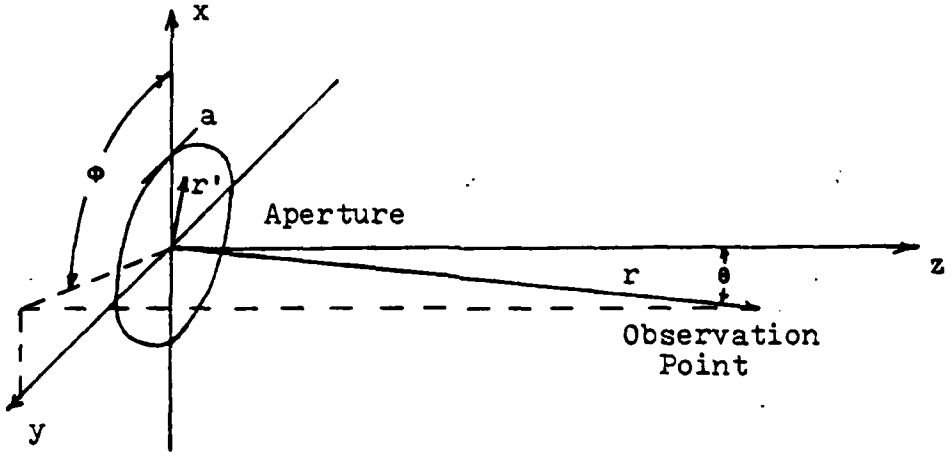

Fig. IV-2. Antenna Aperture Configuration for a Single Parabolic Dish

where $J_1(x)$ and $J_2(x)$ are cylindrical Bessel functions of the first kind, of orders 1 and 2, and $\psi(r)$ is the scalar three-dimensional Greeh's function (Ref 11:420)

$$\psi(r) = \frac{e^{-j\beta r}}{4\pi r}$$

The total field at the observation point is calculated by adding the fields from two antennas: the actual antenna and its image. Since the antenna is close to the ground, the angle of incidence with respect to the ground is very small and the reflection coefficient is -1 (Ref 2:58). This causes the total fields to be zero at the ground. From Figure IV-3 it is seen that the total field in the $\hat{x}$ direction is just the sum of the respective fields from each antenna dotted with the $\hat{x}$ vector.

$$E_{x_{Total}} = (E_{\theta_1}\hat{\theta}_1 - E_{\theta_2}\hat{\theta}_2 + E_{\phi_1}\hat{\phi}_1 - E_{\phi_2}\hat{\phi}_2)\cdot\hat{x}$$

The total electric field can finally be written

$$\bar{E}_T = \hat{x}j\left[\frac{e^{-j\beta r_1}}{4\pi r_1}\frac{2\pi\cos\theta_1}{\sin\theta_1}\left\{aCJ_1(\beta a\sin\theta_1) + \frac{2(1-C)J_2(\beta a\sin\theta_1)}{\beta\sin\theta_1}\right\}\right.$$

$$\left.-\frac{e^{-j\beta r_2}}{4\pi r_2}\frac{2\pi\cos\theta_2}{\sin\theta_2}\left\{aCJ_1(\beta a\sin\theta_2) + \frac{2(1-C)J_2(\beta a\sin\theta_2)}{\beta\sin\theta_2}\right\}\right] \quad \text{(IV-3)}$$

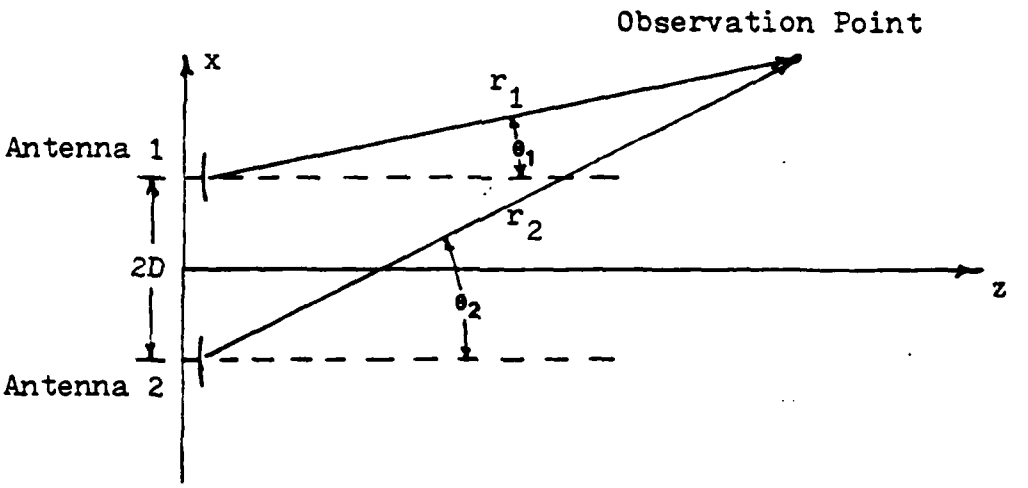

Fig. IV-3. Ground Bounce Range Configuration

Figure IV-4 shows the total field pattern in the vertical plane ($\phi = 0$, $0 < \theta < 10$) for C = .1, a = .9144m(3 ft), λ = .03125m, D = .347m and a tilt angle of .5°.

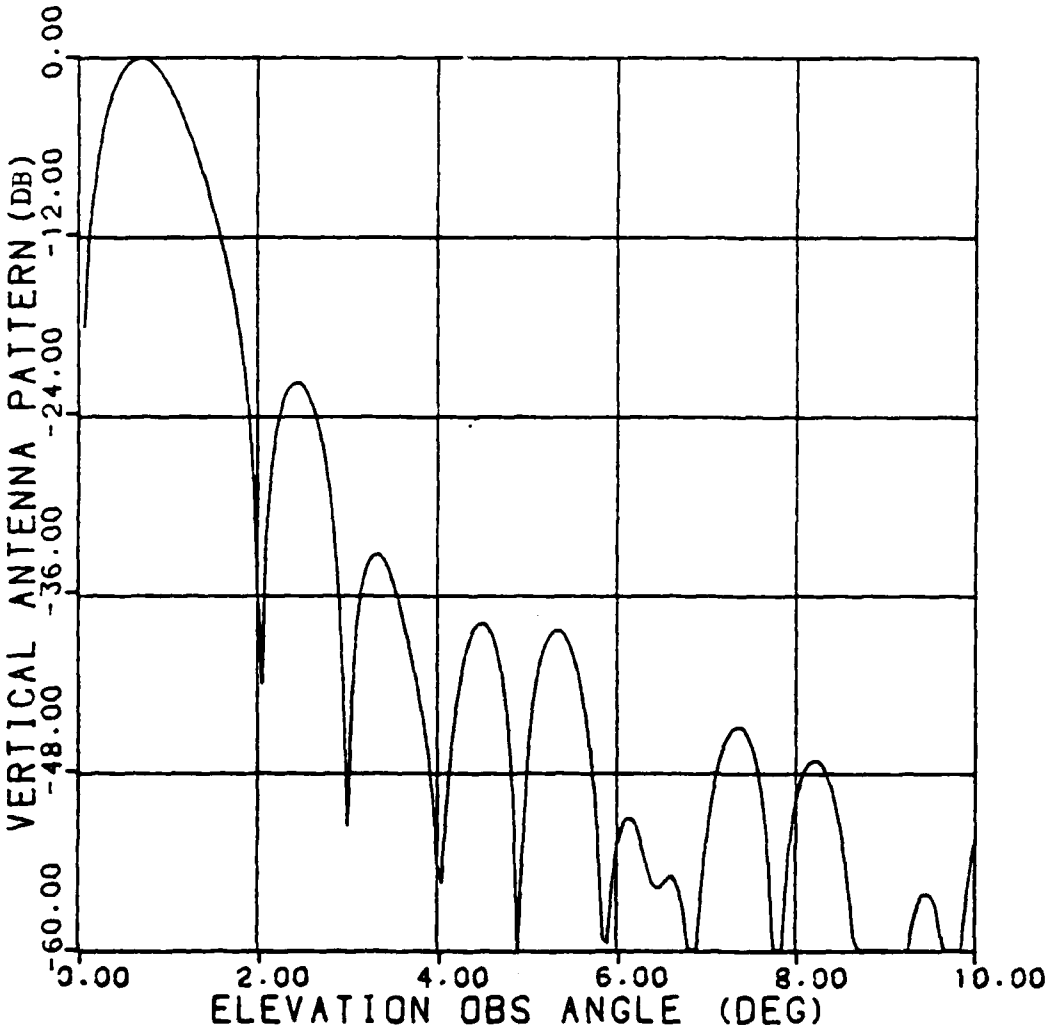

Fig. IV-4. Vertical Pattern Cut of the Ground Bounce Antenna Configuration (C=.1, a=1.828m, D=.347m, θ_T= .5 deg, λ=.03125m)

V. Target Model Description

Introduction

Typical targets today are complex shapes, having many sharp edges, corners, points and rough surfaces. As far as the scattering properties of the target are concerned, the complex target is seen as a scatterer dominated by point scatterers. A reasonable model for a point scattering target is a collection of point scatterers spatially distributed over a defined volume in a random manner.

Description

The targets considered in this thesis are modeled as a distribution of point scatterers along a straight length L. Various spatial distributions of the scatterers along L are used. A uniform spatial distribution is the baseline. A stepped uniform distribution (piecewise constant) is also used. Finally a truncated Gaussian distribution is used (see Figure V-1). The spatial density function is denoted p(y).

The phases of the individually scattered fields are assumed to be uniformly distributed over the range of $0 < \emptyset \leq 2\pi$. The sizes of the individual scatterers are assumed to be constant, $\sigma_i = \sigma$, and each scatterer's position on the target is independent of all the other scatterers. The target is oriented transverse to the RCS measurement antenna so that the antenna always sees a target that has a transverse length L.

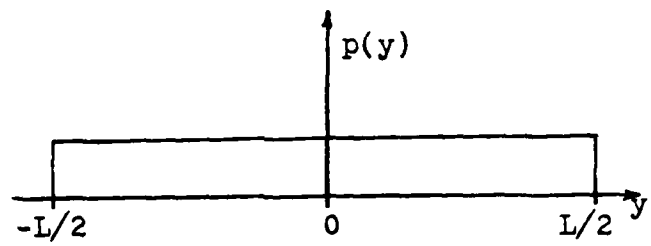

Uniform Spatial Distribution

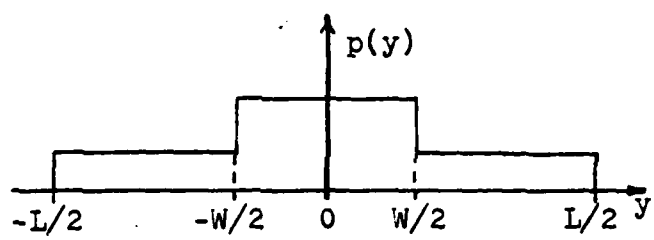

Stepped Distribution

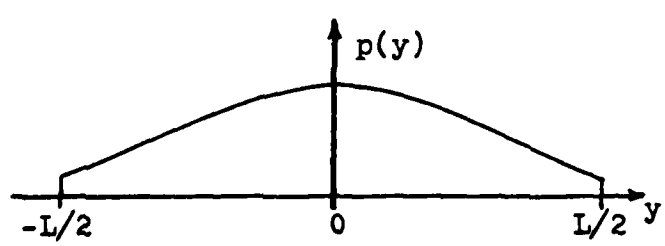

Truncated Gaussian Distribution

Fig. V-1. Spatial Densities of the Point Scatterers Along the Target Length

The reason for keeping the target length transverse to the antenna line of sight is because at any other orientation the antenna essentially sees a projected target of a shorter length.

VI. Statistical Properties of the Fields Scattered from a Distribution of Point Scatterers

Introduction

The following chapter discusses the general amplitude and phase distributions of the field scattered from a collection of point scatterers whose properties are themselves described probabilistically. The general amplitude and phase distributions will then be applied to the specific case of the field scattered from the target modeled as a line of point scatterers. The goal of the following discussion is to develop an expression for the average measured RCS of the target and to take into account the antenna pattern (developed in Chapter IV) and its effect upon the average measured RCS.

The Amplitude Distribution of Multiply Scattered Fields

The electromagnetic field scattered from a random distribution of n point scatterers can be expressed as the sum of the individually scattered fields

$$E_T = Re^{j\emptyset} = \sum_{i=1}^{n} r_i e^{j\emptyset_i} \qquad \text{(VI-1)}$$

where r_i and $\emptyset_i$ are respectively the amplitude and phase of the i^{th} scattered field. The total field can also be expressed as

$$E_T = X + jY = \sum_{i=1}^{n} (x_i + jy_i) \qquad \text{(VI-2)}$$

where

$$\begin{aligned} X &= R\cos\emptyset \\ Y &= R\sin\emptyset \\ x_i &= r_i\cos\emptyset_i \\ y_i &= r_i\sin\emptyset_i \end{aligned} \qquad \text{(VI-3)}$$

At this point no assumptions have been made about the statistical distributions of r_i and $\emptyset_i$. Let the joint probability density function of r_i and $\emptyset_i$ be denoted $p_i(r,\emptyset)$ and all $p_i(r,\emptyset)$ be independent. The independence of the scattered fields is a valid assumption for most practical situations.

The first and second moments of X and Y can be expressed

$$E(X) = \overline{X} = \sum_{i=1}^{n} \int_0^{2\pi}\int_{-\infty}^{\infty} p_i(r,\emptyset)r\cos\emptyset\,dr\,d\emptyset \qquad \text{(VI-4)}$$

$$E(Y) = \overline{Y} = \sum_{i=1}^{n} \int_0^{2\pi}\int_{-\infty}^{\infty} p_i(r,\emptyset)r\sin\emptyset\,dr\,d\emptyset \qquad \text{(VI-5)}$$

The individual terms of Eqs (VI-4) and (VI-5) are denoted

$$\overline{x}_i = \int_0^{2\pi}\int_{-\infty}^{\infty} p_i(r,\emptyset)r\cos\emptyset\,dr\,d\emptyset \qquad \text{(VI-6)}$$

$$\bar{y}_i = \int_0^{2\pi}\int_{-\infty}^{\infty} p_i(r,\phi) r \sin\phi \, dr d\phi \qquad \text{(VI-7)}$$

The variances of X and Y are

$$\text{Var}(X) = S_x = \sum_{i=1}^{n}\left[\int_0^{2\pi}\int_{-\infty}^{\infty} p_i(r,\phi) r^2 \cos^2\phi \, dr d\phi - \bar{x}_i^2\right] \qquad \text{(VI-8)}$$

$$\text{Var}(Y) = S_y = \sum_{i=1}^{n}\left[\int_0^{2\pi}\int_{-\infty}^{\infty} p_i(r,\phi) r^2 \sin^2\phi \, dr d\phi - \bar{y}_i^2\right] \qquad \text{(VI-9)}$$

and the covariance of X and Y is

$$\text{Cov}(X,Y) = \frac{1}{2}\sum_{i=1}^{n}\int_0^{2\pi}\int_{-\infty}^{\infty} p_i(r,\phi) r^2 \sin 2\phi \, dr d\phi +$$

$$\sum_{i=1}^{n}\sum_{\kappa=1}^{n}\int_0^{2\pi}\int_{-\infty}^{\infty} p_i(r,\phi) r \cos\phi \, dr d\phi \int_0^{2\pi}\int_{-\infty}^{\infty} p_\kappa(r,\phi) r \sin\phi \, dr d\phi - \bar{X}\bar{Y}$$

(VI-10)

Now the phases of the scattered fields are assumed to be symmetrically distributed about zero radians. The integrands of

Eqs (VI-5) and (VI-10) are now symmetrically odd functions of $\emptyset$ and integration of (VI-5) and (VI-10) results in (Ref 1:231-232)

$$\bar{Y} = 0 \qquad \text{(VI-11a)}$$

$$\text{Cov}(X,Y) = 0 \qquad \text{(VI-11b)}$$

With these simplifications and the use of the Central Limit Theorem, the joint probability density of X and Y can be calculated. The Central Limit Theorem states that the "probability distribution of a sum of n independent random variables approaches the normal distribution as $n \to \infty$, regardless of the probability distribution of each random variable" (Ref 5:89). The number of scatterers, n, is assumed to be very large and the conditions of the Central Limit Theorem satisfied for most practical applications (Ref 1:232). Using the Central Limit Theorem and the fact that Cov(X,Y) = 0; X and Y are <u>independent normal random variables</u>; the joint density is

$$p(X,Y) = p(X)p(Y) = \frac{1}{2\pi\sqrt{S_x S_y}} \exp\left[\frac{-(X-\bar{X})^2}{2S_x} - \frac{Y^2}{2S_y}\right] \qquad \text{(VI-12)}$$

Transforming X and Y back to polar coordinates and integrating out Ø results in the probability density function of the amplitude of the scattered field (Ref 1:232).

$$p(R) = \frac{R}{2\pi\sqrt{S_x S_y}} \int_0^{2\pi} \exp\left[-\frac{(R\cos\phi - \bar{X})^2}{2S_x} - \frac{R^2\sin^2\phi}{2S_y}\right] d\phi \qquad \text{(VI-13)}$$

The mean scattered power can be derived. First recall that

$$R^2 = X^2 + Y^2$$

The mean scattered power can now be written

$$\begin{aligned} E(R^2) &= E(X^2) + E(Y^2) \\ &= E(X^2) - E(X)^2 + E(Y^2) - E(Y)^2 + E(X)^2 + E(Y)^2 \\ &= S_x + S_y + \bar{X}^2 + \bar{Y}^2 \end{aligned}$$

where E(x) is the expected value of x. Recall $\bar{Y} = 0$, so the mean scattered power is

$$E(R^2) = S_x + S_y + \bar{X}^2 \qquad \text{(VI-14)}$$

Application of the Derived Amplitude Distribution to the Special Case of the Modeled Target

The general statistics of the multiply scattered field are applied to the specific field scattered from the target model. The phase and amplitude ($\emptyset_i$ and r_i) of the individually scattered fields are assumed independent. Also the phases of the scattered fields are assumed to be uniformly distributed as described in the last chapter. The number of scatterers is designated n and each individual scatterer is identically distributed along the length of the target. Since each scatterer's position is identically distributed, all r_i's are also identically distributed.

Using the above simplifications

$$\bar{X} = nE(r)\int_0^{2\pi} \cos\emptyset \left(\frac{1}{2\pi}\right) d\emptyset = 0 \qquad \text{(VI-15)}$$

$$S_x = nE(r^2)\int_0^{2\pi} \cos^2\emptyset \left(\frac{1}{2\pi}\right) d\emptyset - \frac{\bar{X}^2}{n}$$

$$S_x = \frac{nE(r^2)}{2} \qquad \text{(VI-16a)}$$

and in a similar matter

$$S_y = \frac{nE(r^2)}{2} \qquad \text{(VI-16b)}$$

Recall from Eq (VI-14) that the mean scattered power is $E[R^2]$, which is merely equal to the sum of the powers of the individually scattered fields as shown below.

$$E(R^2) = \frac{nE(r^2)}{2} + \frac{nE(r^2)}{2} = nE(r^2) \qquad \text{(VI-17)}$$

The quantities S_x and S_y can now be substituted into Eq (VI-13), resulting in (Ref 1:238)

$$p(R) = \frac{2R}{nE(r^2)} \exp\left[\frac{-R^2}{nE(r^2)}\right] \qquad \text{(VI-18)}$$

Recall that R is the magnitude of the total field scattered from the target. Eq (VI-18) is a Rayleigh distribution. For the case when the scatterers do not all have the same spatial distributions (Ref 1:238)

$$S_x = S_y = \frac{1}{2}\sum_{i=1}^{n} E(r_i^2) \qquad \text{(VI-19)}$$

and

$$p(R) = \frac{2R}{\sum_{i=1}^{n} E(r_i^2)} \exp\left[\frac{-R^2}{\sum_{i=1}^{n} E(r_i^2)}\right] \qquad \text{(VI-20)}$$

At this point no assumptions have been made concerning the amplitude distributions of the individual scattered fields, r_i's. The scatterers are assumed to be in an antenna field pattern. It is the field pattern which dictates the magnitude of the incident field at each scattering point on the target. It can be easily seen that

$$r_i \propto |F(\theta_i, \phi_i)| \qquad \text{(VI-21)}$$

where $F(\theta,\phi)$ is the normalized antenna pattern and θ and ϕ are spherical coordinates relative to the antenna axis. The coordinates θ and ϕ are random variables and are related to the random positions of the point scatterers along the length of the target. Using Eq (VI-21) in conjunction with Eq (VI-17), the mean scattered power is proportional to

$$E(R^2) = nE(r^2) \propto nE\left[|F(\theta,\phi)|^2 \right] \qquad \text{(VI-22)}$$

The mean power received by the RCS measurement antenna due to the scattered power density is

$$E(P_{rec}) = E(S_s A_e) \qquad \text{(VI-23)}$$

where

S_s is the scattered power density
A_e is the effective area of the antenna.

The effective area of the antenna is defined

$$A_e(\theta,\phi) = \frac{\lambda^2}{4\pi} G(\theta,\phi) \qquad \text{(VI-24)}$$

where $G(\theta,\phi)$ is the gain of the antenna. Further simplification of A_e results in (Ref 11: 36-38)

$$A_e(\theta,\phi) = \frac{\lambda^2}{4\pi} \frac{|F(\theta,\phi)|^2}{\frac{1}{4\pi}\int_0^{2\pi}\int_0^{\pi}|F(\theta,\phi)|^2 \sin\theta d\theta d\phi}$$

$$= \frac{\lambda^2}{4\pi\Omega_A} |F(\theta,\phi)|^2 \qquad \text{(VI-25)}$$

Using Eq (VI-25) in Eq (VI-23) gives

$$E(P_{rec}) = E\left[\frac{S_s \lambda^2}{4\pi\Omega_A} |F(\theta,\phi)|^2\right] \qquad \text{(VI-26)}$$

Recall from Eq (VI-22) that the mean of the scattered power density is proportional to $E[|F(\theta,\phi)|^2]$. Putting this into Eq (VI-26) gives

$$E(P_{rec}) \propto E\left[|F(\theta,\phi)|^4\right] \qquad \text{(VI-27)}$$

The radar range equation relates the measured RCS to the received power. The radar range equation is shown below (Ref 10:4).

$$P_{rec} = \frac{P_t \lambda^2 G^2 \sigma_m}{(4\pi)^3 R^4} \qquad \text{(VI-28)}$$

Eq (VI-28) shows that the power received is proportional to the RCS of the target. Using Eq (VI-28) in (VI-27) results in

$$(\text{Measured RCS})_{avg} = \bar{\sigma}_m \propto E\left[|F(\theta,\phi)|^4\right]$$

$$\propto \overline{|F(\theta,\phi)|^4} \qquad \text{(VI-29)}$$

Summary

The general statistics of the field scattered from a random distribution of point scatterers is reviewed. These general statistics are applied to the specific field scattered from the modeled target. Using the characteristics of the modeled target, the magnitude of the scattered field is found to be Rayleigh distributed and the total power of the scattered field is found to be the sum of the powers of the individually

scattered fields. Using this fact, a relationship between the measured RCS and the antenna pattern is established. This relationship is seen in Eq (VI-29), and is the relationship needed to study the effects of range reduction on RCS measurements.

VII. Approximations and Simulation Techniques

Introduction

One of the main goals discussed in Chapter I is examining the effect of range reduction on RCS measurements for the target dominated by point scatterers. The following chapter reviews the approximation and simulation techniques used to examine the effect of range reduction on RCS measurements. Before getting into the approximation and simulation techniques recall the modeled target and the various spatial distributions of the point scatterers described in Chapter V. Also recall from Eq (VI-29) that the measured RCS was found to be proportional to the mean of the antenna pattern factor raised to the fourth power,

$$E(\sigma_m) = K\,\overline{F^4(\theta,\phi)}$$

Before proceeding and discussing the approximation and simulation techniques, the next section reviews the RCS measurement configuration.

Target and Antenna Configuration

The physical geometry of the RCS measurement range can be seen in Figure VII-1. This geometry closely resembles the measurement range at the RAT SCAT facility. The measurement range is a ground bounce range, utilizing the effective image

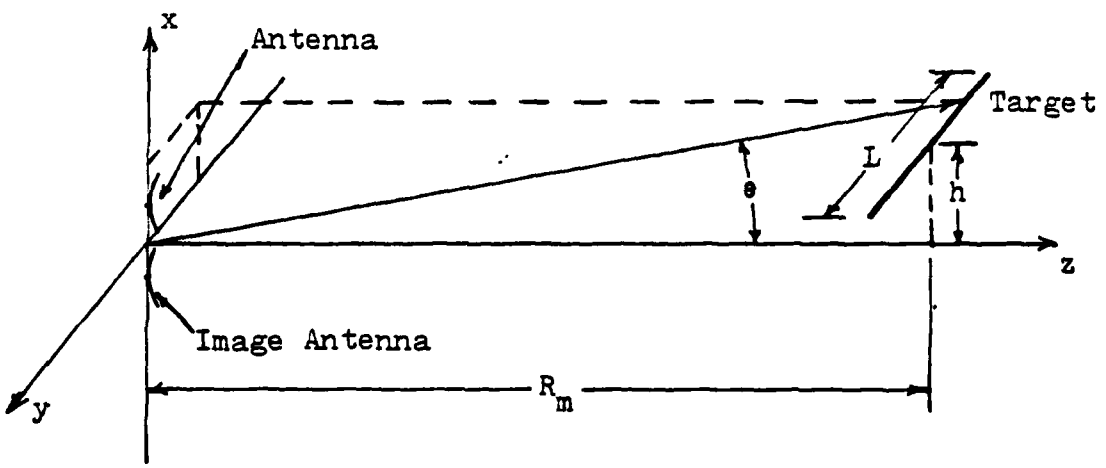

Fig. VII-1. RCS Measurement Range Configuration

of the radar antenna below the ground. R_m is the ground range out to the target and h is the height of the target above the ground. For the measurement range discussed here, the antenna is a parabolic reflector dish of radius a. The radiated fields were found using aperture integration (see Chapter IV). The target is placed in the main lobe of the combined antenna pattern (antenna and its image), and as the target range is reduced, the height of the target, h, is varied to cause the target to stay in the main lobe of the antenna pattern. As seen in Figure IV-4, the main lobe of the antenna pattern is at an elevation of .5 degrees relative to the ground for a = .9144 meters and a frequency of 9.6 GHz. To keep the target in the main lobe of the antenna, all that is required is to keep the inverse tangent of h/R_m equal to .5 degrees.

The point scatterers are distributed spatially along the length of the target. Since the target is always transverse to the antenna and also horizontal, the spatial distribution of the scatterers are only along a line parallel to the y axis (see Figure VII-1). The probability density function describing the spatial distribution of the scatterers is denoted p(y) for $-L/2 < y < L/2$. The other coordinates, x and z, are constant for a particular target range. The task now is to find the mean of the measured RCS, which is proportional to $\overline{F^4(\theta,\emptyset)}$. The task is not simple to perform analytically since $F(\theta,\emptyset)$ is a complicated function of θ and $\emptyset$ and in turn θ and $\emptyset$ are complicated functions of x, y and z. The task is also

further complicated due to the antenna pattern being the sum of two field patterns: the antenna and its image.

Monte-Carlo Method

Finding $\overline{F^4(\theta,\phi)}$ analytically is beyond the scope of this thesis due to the complexity of $F(\theta,\phi)$. One method of approximating $\overline{F^4(\theta,\phi)}$ is to perform many numerical experiments and computing the mean as follows (Ref 8:138):

$$\overline{F^4(\theta,\phi)} \cong \frac{F^4(\theta_1,\phi_1) + F^4(\theta_2,\phi_2) + \cdots + F^4(\theta_N,\phi_N)}{N} \qquad \text{(VII-1)}$$

where $F^4(\theta_k,\phi_k)$ is a numerical result and N is the number of experiments. Uniform and Gaussian random number generators are used to generate the random samples needed for the numerical experiments. The output from the number generators are scaled and translated as needed to simulate a random position sampled from the length of the target. The probability density, p(y), is thus simulated. Recall that different p(y)'s are used: a uniform, a stepped uniform and a truncated Gaussian.

Once a sample is selected from an appropriately scaled and translated random number generator, the value of the antenna pattern factor is calculated for the corresponding position, y. This value is raised to the fourth power and added to the results of the other numerical experiments. With many samples, $\overline{F^4(\theta,\phi)}$ can be closely approximated. All of the numerical

experiments are conducted using a computer to generate the random numbers and to also calculate the mean. The range, R_m, can be varied to examine the effect on the average measured RCS. The changes in $\overline{F^4(\theta,\phi)}$, as the range is varied, are equal to the relative changes of the measured RCS. It is the relative changes of the measured RCS that are of interest.

It is also desirable to analytically calculate the mean of the measured RCS. In the following section, the main lobe of the antenna pattern is approximated by a Gaussian shape. This shape simplifies calculations for the mean of the measured RCS and avoids the use of a computer to generate samples.

Analytical Method

The antenna field derived in Chapter IV is approximated in the main lobe by using a Gaussian shaped lobe. As shown in Figure VII-2, the Gaussian shape is a very good approximation out to the -3 db points. The Gaussian antenna pattern is expressed (Ref 3:268)

$$F(\theta) = \exp\left[-2\ln 2\left[\frac{\theta}{\theta_3}\right]^2\right] \qquad \text{(VII-2)}$$

where θ is the spherical coordinate relative to the antenna bore sight axis. The constant θ_3 is the half power beamwidth of the Gaussian pattern. The constant, θ_3, is set equal to the half power (HP) beamwidth of the antenna field pattern derived in Chapter IV. The HP beamwidth is a function of the antenna

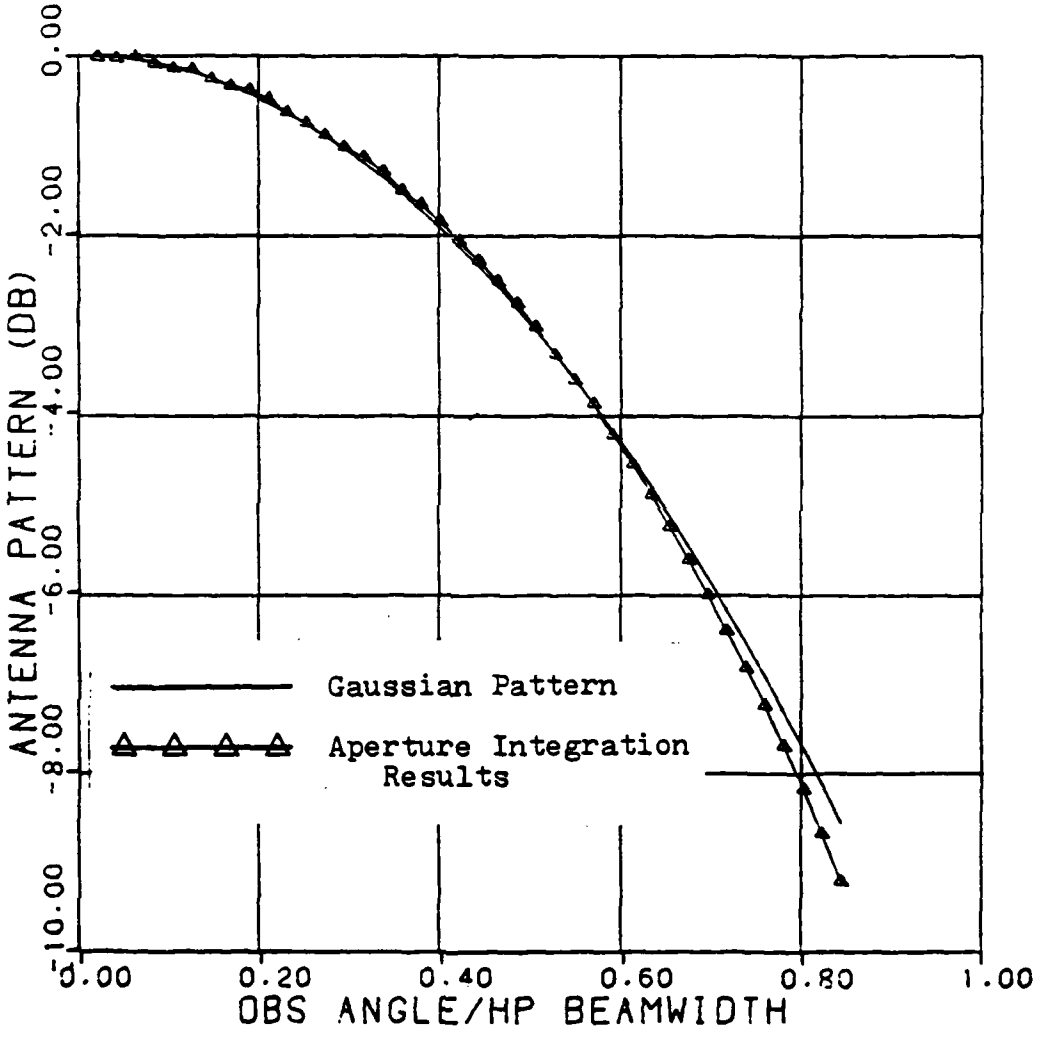

Fig. VII-2. Comparison of the Horizontal Antenna Pattern and the Gaussian Pattern(C=.1, a=1.828m, D=.347m, θ_T=.5 deg, =.03125m)

parameters, such as the aperture illumination pedestal height, the size of the parabolic dish and the frequency of operation. Recall that the derived field pattern is a combination of the fields from the antenna and its image, and this combination complicates finding the HP beamwidth.

Since the target is always horizontal to the ground, the HP beamwidth is only needed in the horizontal dimension. From antenna theory it is known that the antenna pattern of a linear one dimensional array is equal to the antenna pattern of a single element of the array in a cut perpendicular to the array length. The parabolic dish antenna and its image below the ground can be thought of as a one dimensional array of two elements. The antenna pattern in the horizontal dimension is equal to the antenna pattern of a single parabolic dish. The HP beamwidth in the horizonal dimension can now be found since the problem for the single parabolic reflector antenna has already been solved. Figure VII-3 shows the relationship between the HP beamwidth and the aperture illumination pedestal height (Ref 9:85).

Once the HP beamwidth is known, it can be used in Eq (VII-2). Remember that θ is related to the random variable y (see Figure VII-4). The random variable θ is equal to

$$\theta = \tan^{-1}(y/R_m) \qquad \text{(VII-3)}$$

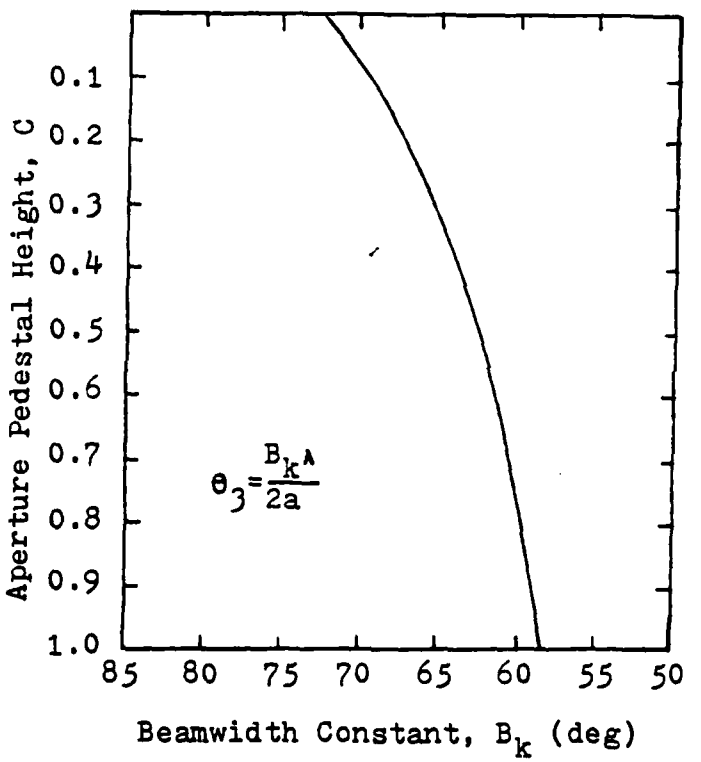

Fig. VII-3. 3 db Beamwidth of Circular Aperture

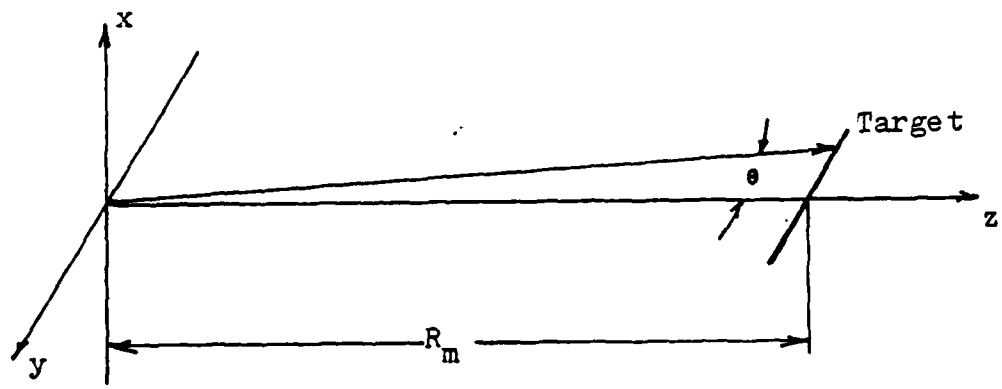

Fig. VII-4. Relationship of θ to y using the Gaussian Pattern

which can be approximated by

$$\theta \cong \frac{y}{R_m} \qquad \text{(VII-4)}$$

for $R_m >> y$. Using Eq (VII-4) in Eq (VII-2) results in

$$F(y) = \exp\left[\frac{-2\ln 2 y^2}{\theta_3^2 R_m^2}\right] \qquad \text{(VII-5)}$$

The mean of $F^4(y)$ can now be expressed

$$\overline{F^4(y)} = \int_{-L/2}^{L/2} \left\{\exp\left[\frac{-2\ln 2 y^2}{\theta_3^2 R_m^2}\right]\right\}^4 p(y)dy$$

$$= \int_{-L/2}^{L/2} \exp\left[\frac{-8\ln 2 y^2}{\theta_3^2 R_m^2}\right] p(y)dy \qquad \text{(VII-6)}$$

<u>Eq (VII-6) is a function of R_m and is proportional to the measured RCS. Eq (VII-6) is the analytical expression needed to examine the effects of range reduction on RCS measurements.</u>

Summary

Two methods have been introduced for finding $\overline{F^4(\theta,\emptyset)}$. The Monte-Carlo method is the first method discussed. The Monte-Carlo method is a numerical simulation. The analytical method is the second method discussed and is derived using an approximation of the antenna main lobe pattern. The analytical method resulted in Eq (VII-6). Both of these methods will be used in the next chapter to examine the effects of range reduction on RCS measurements.

VIII. Results of the Monte-Carlo Simulations and Gaussian Antenna Pattern Approximation

Introduction

The two methods outlined in the previous chapter, the Monte-Carlo simulation and the Gaussian antenna pattern approximation, are used to examine the effects of range reduction on RCS measurements. These methods are used for the various target models outlined in Chapter V. The results that are obtained using the two methods do not give the actual average measured RCS, but results which are proportional to the average measured RCS. Since we are only interested in the relative changes of the average measured RCS as the range is varied, the true average RCS measurement of the target is not needed.

The first target examined is the uniformly distributed target; next, the stepped uniform target (piecewise constant) and finally, the truncated Gaussian target. The uniform target will be used as a baseline to compare the results of the other targets.

Uniformly Distributed Target

The target considered in this section consists of many point scatterers uniformly distributed along the length of the target (as outlined in Chapter V). A comparison of the Monte-Carlo (numerical) and the Gaussian antenna pattern

approximation (analytical) results will be made. Recall that the average measured RCS is proportional to $E[F^4(\theta,\emptyset)]$, and by using Eq (VII-6)

$$\overline{\sigma_m} \propto \int_{-L/2}^{L/2} \exp\left[\frac{-8\ln 2 y^2}{\theta_3^2 R_m^2}\right] p(y)dy \qquad \text{(VIII-1)}$$

The density function, p(y), is equal to 1/L for the uniformly distributed target. By letting $\overline{\sigma_o}$ equal the true average RCS obtained in the far field limit, the average measured RCS normalized by $\overline{\sigma_o}$ is now equal to the right side of Eq (VIII-1), and Eq (VIII-1) reduces to

$$\frac{\overline{\sigma_m}}{\overline{\sigma_o}} = \frac{\sqrt{2\pi}\theta_3 R_m}{2L\sqrt{\ln 2}} \operatorname{erf}\left[\frac{2L\sqrt{\ln 2}}{\theta_3 R_m}\right] \qquad \text{(VIII-2)}$$

where R_m is the target range, θ_3 is the 3 db beamwidth and the error function is given by (Ref 8:64)

$$\operatorname{erf}(\tau) = \int_0^{\tau} \frac{1}{\sqrt{2\pi}} \exp(-x^2/2)dx$$

To show that there is a very good agreement between the Monte-Carlo results and the analytical results [Eq (VIII-2)], an example is shown. Assuming an 18.29 meter (60 ft.) target and an antenna 3 db beamwidth of 1.18 degrees; Figure VIII-1 shows a graph of $\overline{\sigma_m}/\overline{\sigma_o}$ versus range. Very good agreement between the two methods is evident. As seen in Figure VIII-1, RCS measurements can be made at ranges down to approximately 1200 meters with less than 1 db deviation from the true far field RCS measurement.

It was noted in the introduction of this chapter that the uniformly distributed target is used as a baseline for comparison of the other target models. It is desirable to be able to relate a specific target of length L, having any spatial distribution, to an equivalent length target of L', having a uniform spatial ditribution. If the specific target is already characterized by a uniform spatial distribution, then L' = L. However, for the stepped and truncated Gaussian spatial distributions, L' generally will not be equal to L. To facilitate the use of the uniformly distributed target as a baseline target for comparison of the other targets, Eq (VIII-2) is generalized. Defining a normalized range

$$\frac{R_m \theta_3}{L} = H \qquad \text{(VIII-3)}$$

Eq (VIII-2) becomes

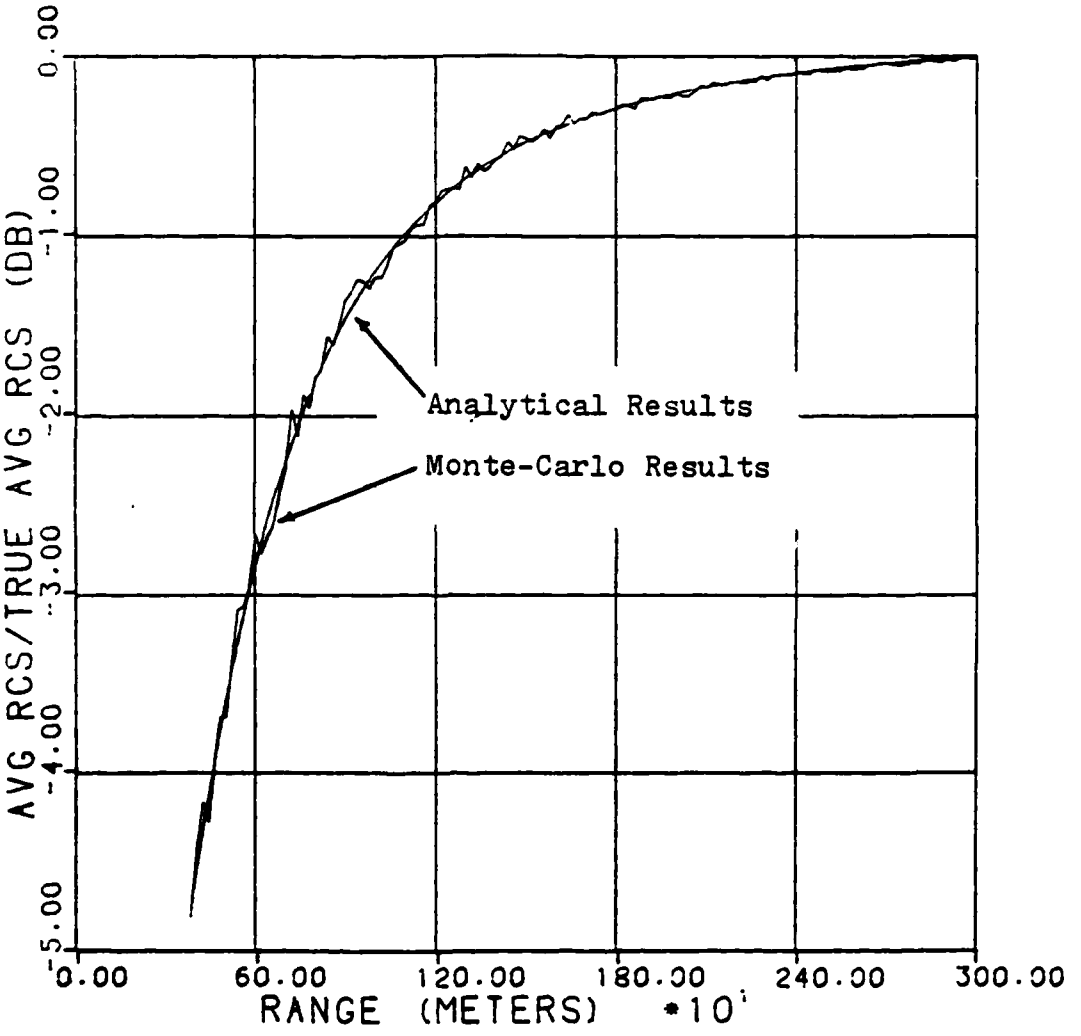

Fig. VIII-1. Average Measured RCS Normalized by the True Average RCS versus Range for an Uniformly Distributed Target (L=18.28m, 3 db Beamwidth=1.18 deg)

$$\frac{\bar{\sigma}_m}{\sigma_o} = \frac{\sqrt{\pi}H}{\sqrt{2\ln 2}} \operatorname{erf}\left[\frac{2\sqrt{\ln 2}}{H}\right] \qquad \text{(VIII-4)}$$

Eq (VIII-4) is plotted in Figure VIII-2 . By specifying a 3 db beamwidth, a target length, (uniformly distributed) and an allowable RCS measurement loss, a minimum measurement range can be obtained from Figure VIII-2.

Stepped Distributed Target

The targets characterized by the stepped spatial distributions are shown in Figure VIII-3. The probability density in Figure VIII-3a, $p_a(y)$, has x as a parameter. The parameter x is the probability that a point scatterer will fall within the range specified by w. For example, if x = .5, there is a fifty percent chance that the point scatterer will be located on the y axis between -w/2 and w/2. The probability density in Figure VIII-3b has m as a parameter. The parameter m specifies the ratio of $p_b(y)$ for $-w/2 < y < w/2$ to $p_b(y)$ for $-L/2 < y < -w/2$ or $w/2 < y < 1/2$.

Again using the result from the previous chapter, the normalized average RCS is

$$\frac{\bar{\sigma}_m}{\sigma_o} = \int_{-L/2}^{L/2} \exp\left[\frac{-8\ln 2 y^2}{\theta_3^2 R_m^2}\right] p(y)dy \qquad \text{(VIII-5)}$$

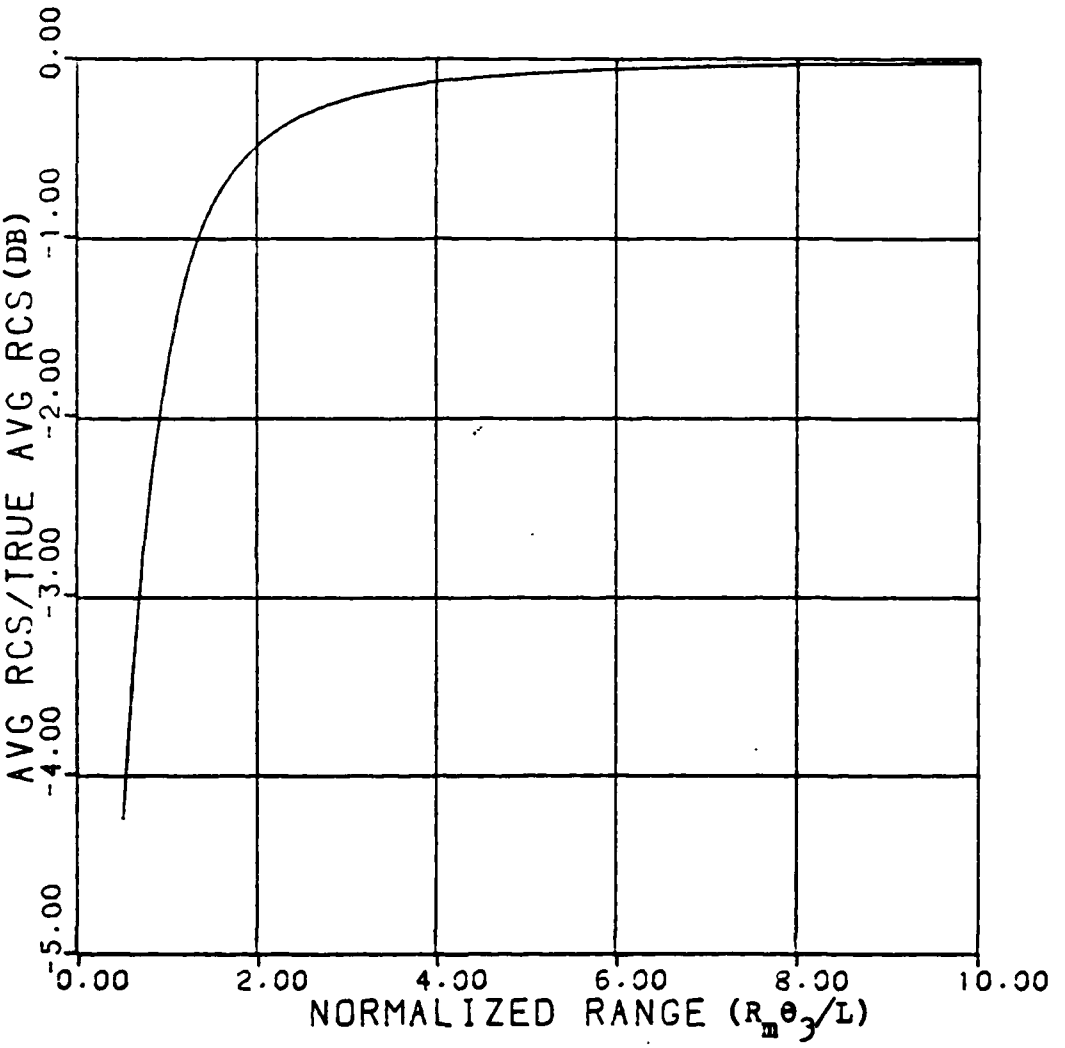

Fig. VIII-2. Average Measured RCS Normalized by the True Average RCS versus Normalized Range($R_m\theta_3/L$) for an Uniformly Distributed Target

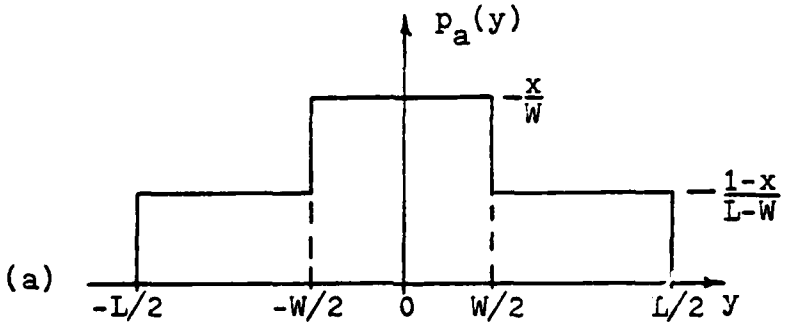

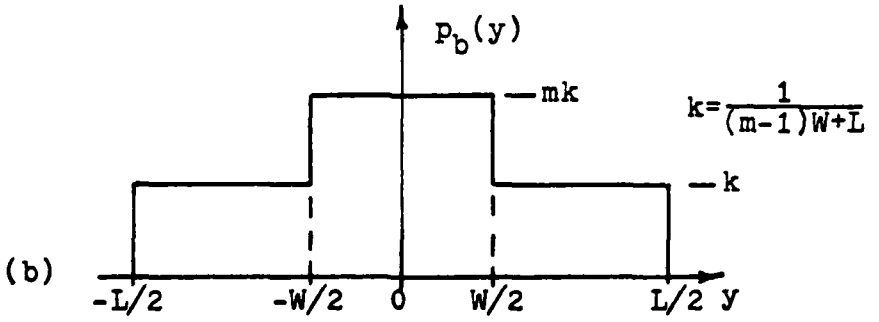

Fig. VIII-3. Spatial Densities of the Point Scatterers along the Target Length($p_a(y)$ and $p_b(y)$)

and substituting $p_a(y)$ in Eq (VIII-5) gives

$$\left[\frac{\bar{\sigma}_m}{\bar{\sigma}_o}\right]_a = \frac{\sqrt{\pi}\theta_3 R_m}{\sqrt{2\ln 2}(L-W)}\left\{\frac{xL-W}{W}\text{erf}\left[\frac{2W\sqrt{\ln 2}}{\theta_3 R_m}\right] + (1-x)\text{erf}\left[\frac{2L\sqrt{\ln 2}}{\theta_3 R_m}\right]\right\} \quad \text{(VIII-6)}$$

Also substituting $p_b(y)$ in Eq (VIII-5) gives

$$\left[\frac{\bar{\sigma}_m}{\bar{\sigma}_o}\right]_b = \frac{\sqrt{\pi}\theta_3 R_m}{\sqrt{2\ln 2}((m-1)W-L)}\left\{(m-1)\text{erf}\left[\frac{2W\sqrt{\ln 2}}{\theta_3 R_m}\right] + \text{erf}\left[\frac{2L\sqrt{\ln 2}}{\theta_3 R_m}\right]\right\} \quad \text{(VIII-7)}$$

These analytical results [Eqs (VIII-6) and (VIII-7)] can be compared to the results from the Monte-Carlo method. A specific example, illustrating the agreement, is seen in Figure VIII-4.

At this point it is desirable to derive an "equivalent length" target that will give approximately the same RCS variation versus range as the target described by $p_a(y)$ or $p_b(y)$. Mathematically this means solving the following expression [see Eq (VII-6)].

$$\int_{-L/2}^{L/2} \exp\left[\frac{-8\ln 2 y^2}{\theta_3^2 R_m^2}\right] p_{a,b}(y)dy = \int_{-L'/2}^{L'/2} \exp\left[\frac{-8\ln 2 y^2}{\theta_3^2 R_m^2}\right]\frac{1}{L'}dy \quad \text{(VIII-8)}$$

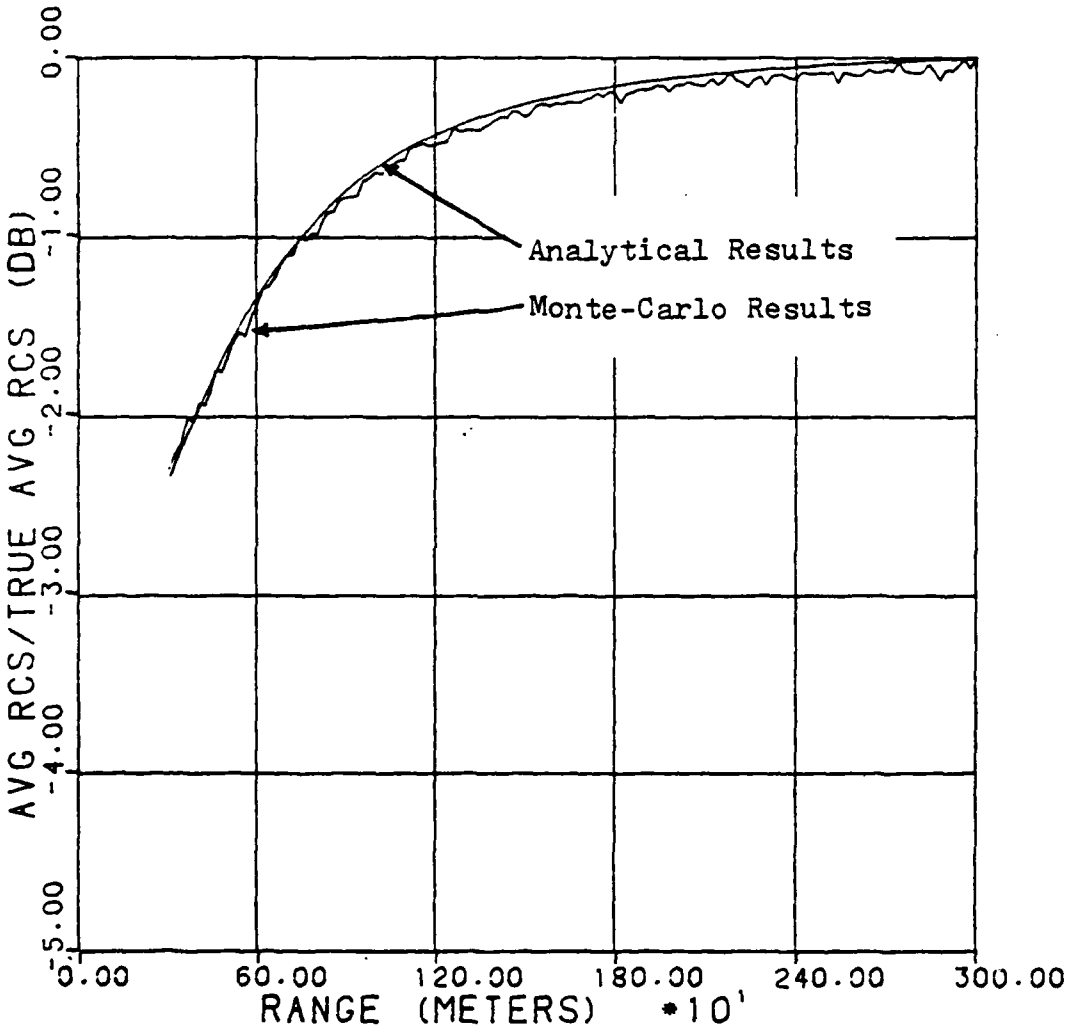

Fig. VIII-4. Average Measured RCS Normalized by the True RCS versus Range for a Stepped Distribution ($p_a(y)$, x=1/2, L=18.28m, W=1.828m, 3 db Beamwidth=1.18 deg)

where L' is the length of the equivalent length target. If the Gaussian pattern is approximated as

$$\exp\left[\frac{-8\ln 2y^2}{\theta_3^2 R_m^2}\right] = 1 - \frac{8\ln 2y^2}{\theta_3^2 R_m^2} \qquad \text{(VIII-9)}$$

then

$$\int_{-L/2}^{L/2}\left[1 - \frac{8\ln 2y^2}{\theta_3^2 R_m^2}\right] p_{a,b}(y)dy = \int_{-L'/2}^{L'/2}\left[1 - \frac{8\ln 2y^2}{\theta_3^2 R_m^2}\right]\frac{1}{L'}dy$$

$$\int_{-L/2}^{L/2} y^2 p_{a,b}(y)dy = \int_{-L'/2}^{L'/2}\frac{y^2}{L'}dy$$

$$E_{a,b}(y^2) = \frac{L'^2}{12}$$

Solving for L' results in

$$L'_a = \sqrt{12E_a(y^2)} \qquad \text{(VIII-10a)}$$

$$L'_b = \sqrt{12E_b(y^2)} \qquad \text{(VIII-10b)}$$

where

$$E_x(y^2) = \int y^2 p_x(y)dy$$

Evaluating Eqs (VIII-10a) and (VIII-10b) results in

$$L'_a = L\sqrt{\frac{(\frac{W}{L})^2(x-\frac{W}{L}) + (1-x)}{1 - \frac{W}{L}}} \qquad \text{(VIII-11a)}$$

$$L'_b = L\sqrt{\frac{(\frac{W}{L})^3(m-1) + 1}{(\frac{W}{L})(m-1) + 1}} \qquad \text{(VIII-11b)}$$

Care must be taken in using the approximation shown in Eq (VIII-9). The quantity $H = R_m\theta_3/L$ should be greater than 1.665 to achieve an error of less than eighteen percent for the approximation. Eqs (VIII-11a) and (VIII-11b) are plotted in Figures VIII-5 and VIII-6 for various values of x and m. Note that the equivalent length, L', decreases as the density of point scatterers increases in the center of the target.

Once a target is characterized by $p_a(y)$ or $p_b(y)$, an equivalent target can be obtained from Eq (VIII-11), and Figure VIII-2 can be used to relate $\overline{\sigma_m}/\overline{\sigma_o}$ to the normalized range $(r_m\theta_3/L')$. Shown in Figures VIII-7 through VIII-14 are some comparisons of $\overline{\sigma_m}/\overline{\sigma_o}$ versus range for a specific target and its equivalent length target. From the graphs, error is evident as

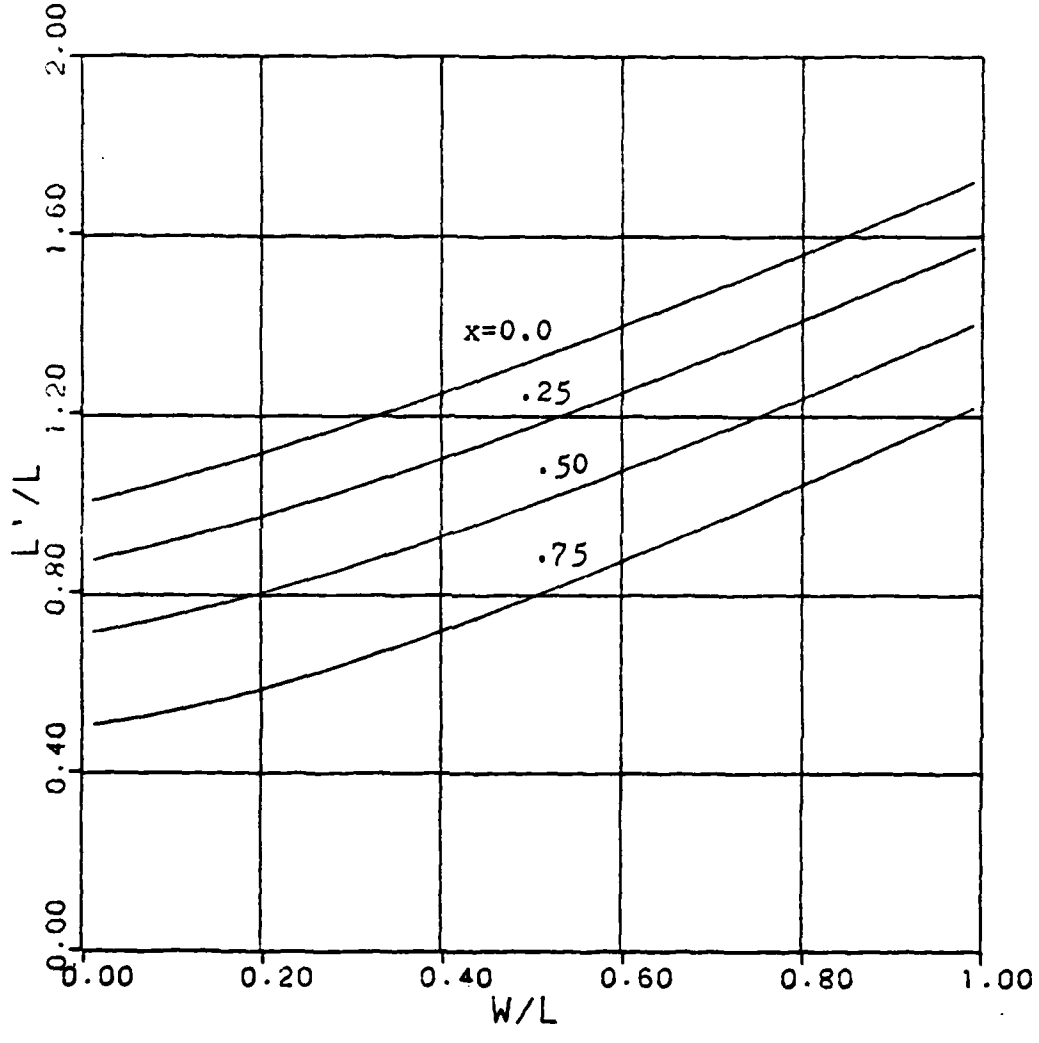

Fig. VIII-5. L'_a/L versus W/L for varicus values of x

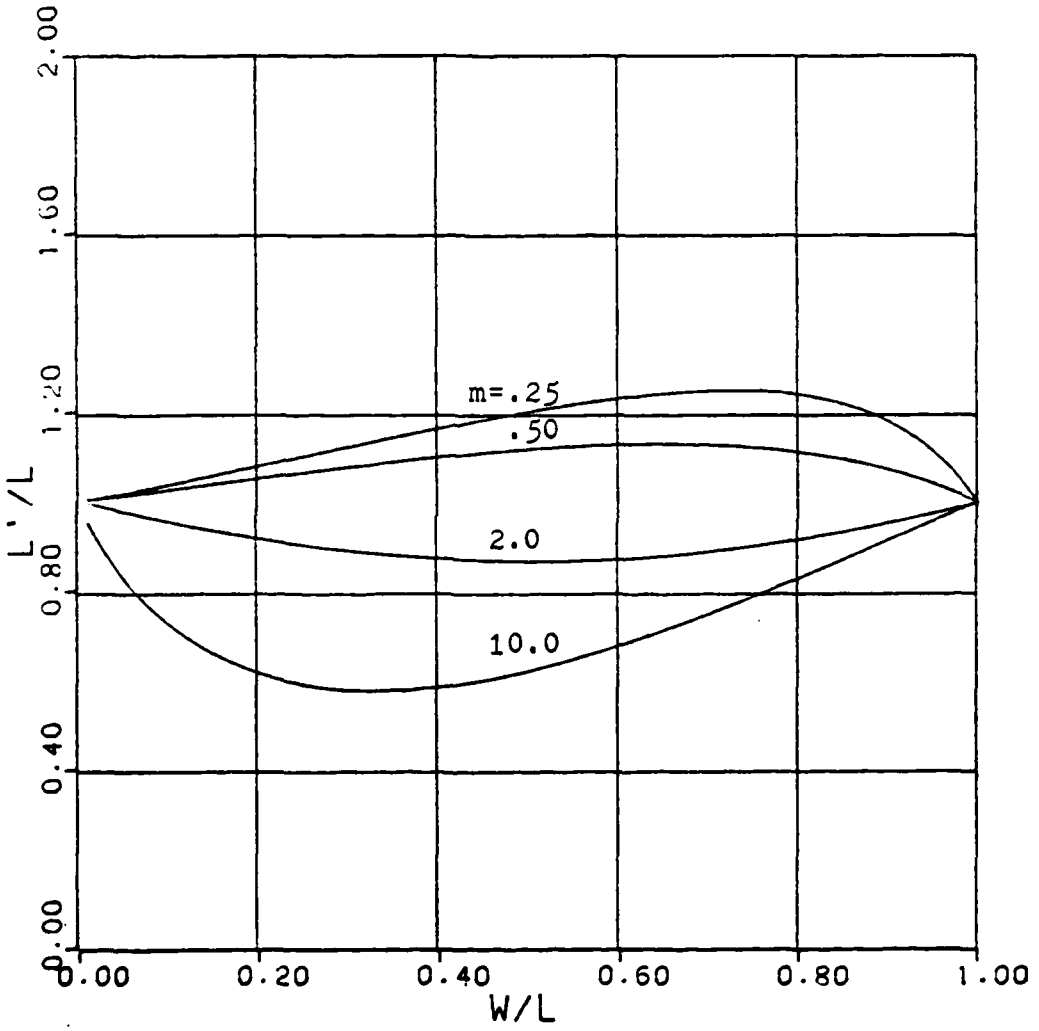

Fig. VIII-6. L_b'/L versus W/L for various values of m

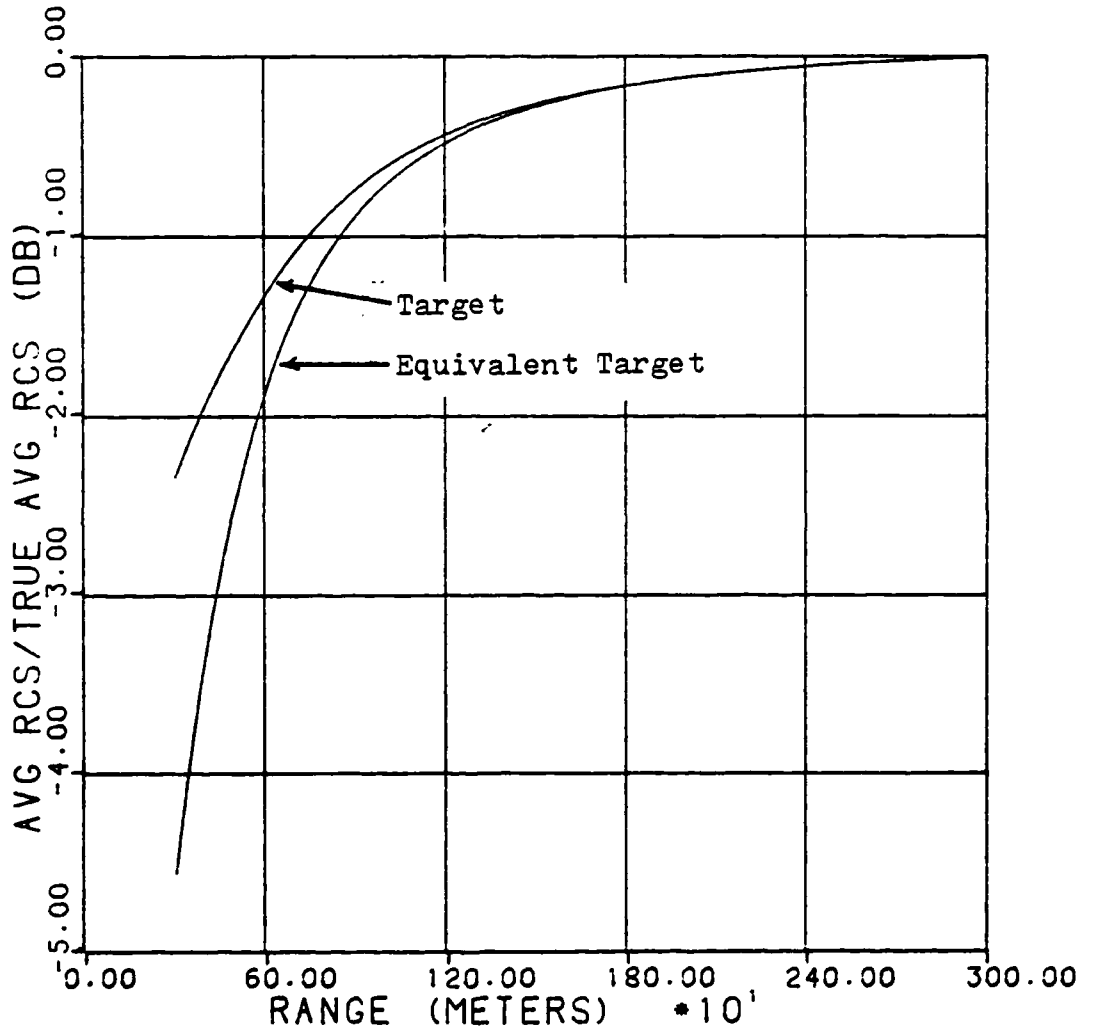

Fig. VIII-7. Comparison of Average RCS Variation for a Specific Target and it's Equivalent Length Target(Target Distribution-$p_a(y)$, x=1/2, L=18.28m, W=1.828m; Equivalent Target-L_a'=13.68m; θ_3=1.18 deg)

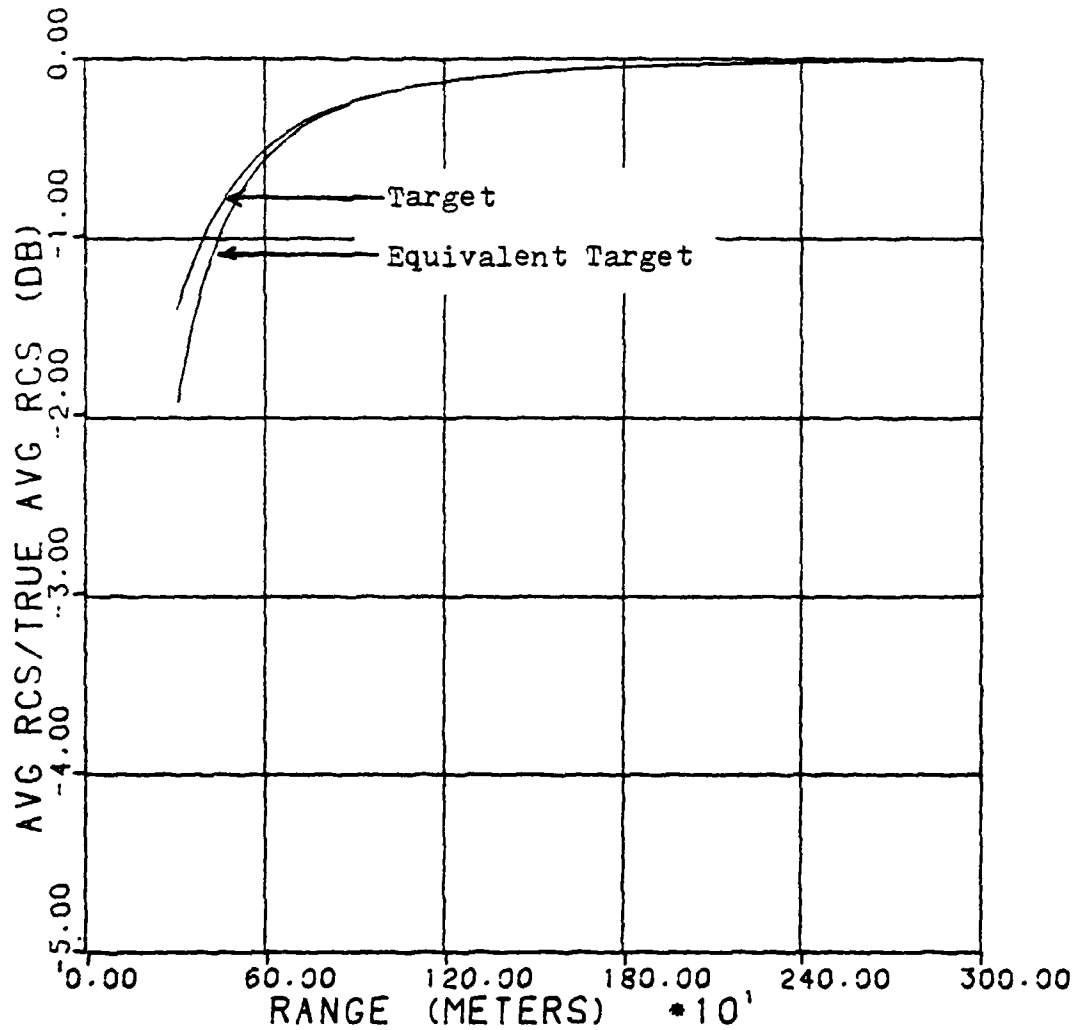

Fig. VIII-8. Comparison of Average RCS Variation for a Specific Target and it's Equivalent Length Target(Target Distribution-$p_a(y)$, x=1/2, L=9.144m, W=.9144m; Equivalent Target-L_a'=6.84m; θ_3=1.18 deg)

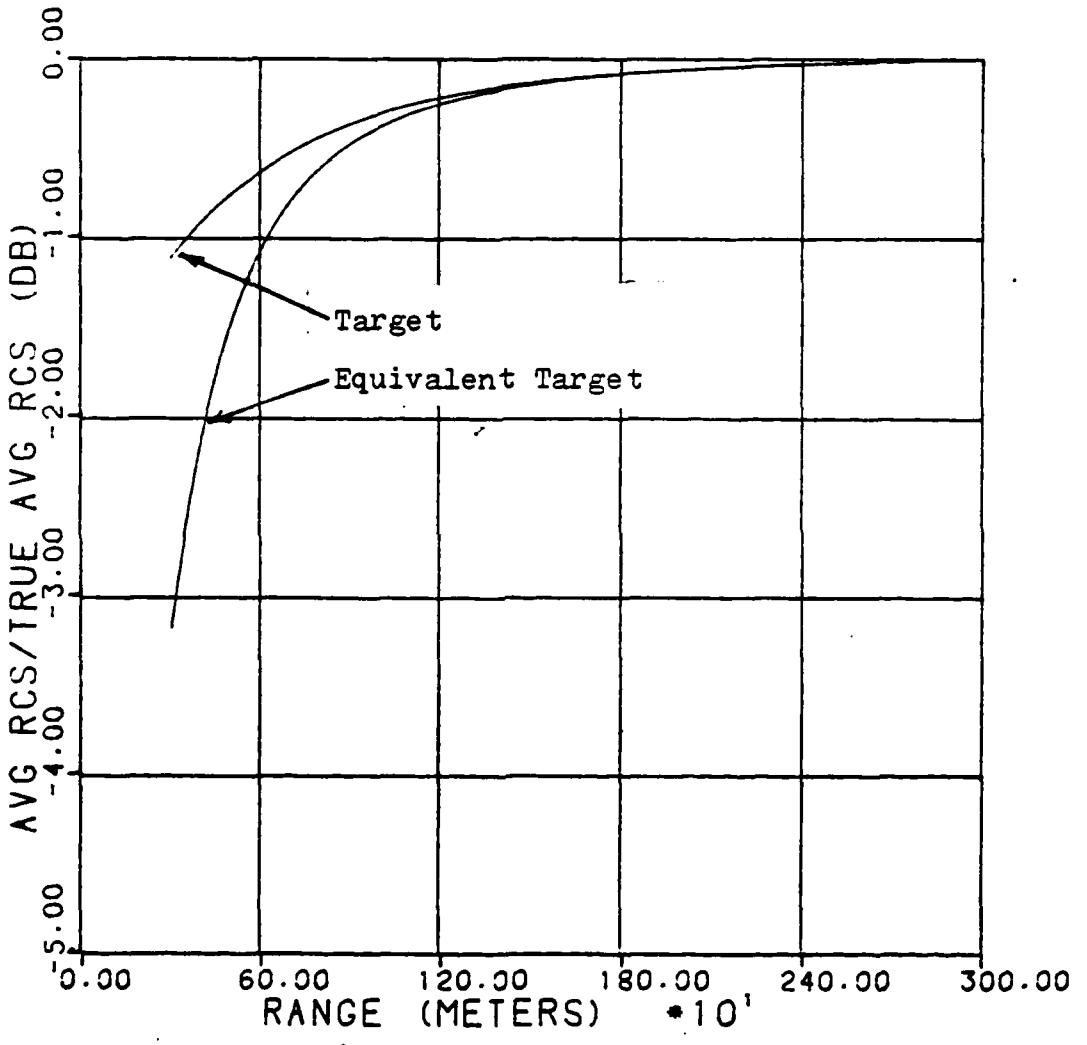

Fig. VIII-9. Comparison of Average RCS Variation for a Specific Target and it's Equivalent Length Target(Target Distribution-$p_a(y)$,x=3/4, L=18.28m, W=1.828m; Equivalent Length-L'_a=9.76m; θ_3=1.18 deg)

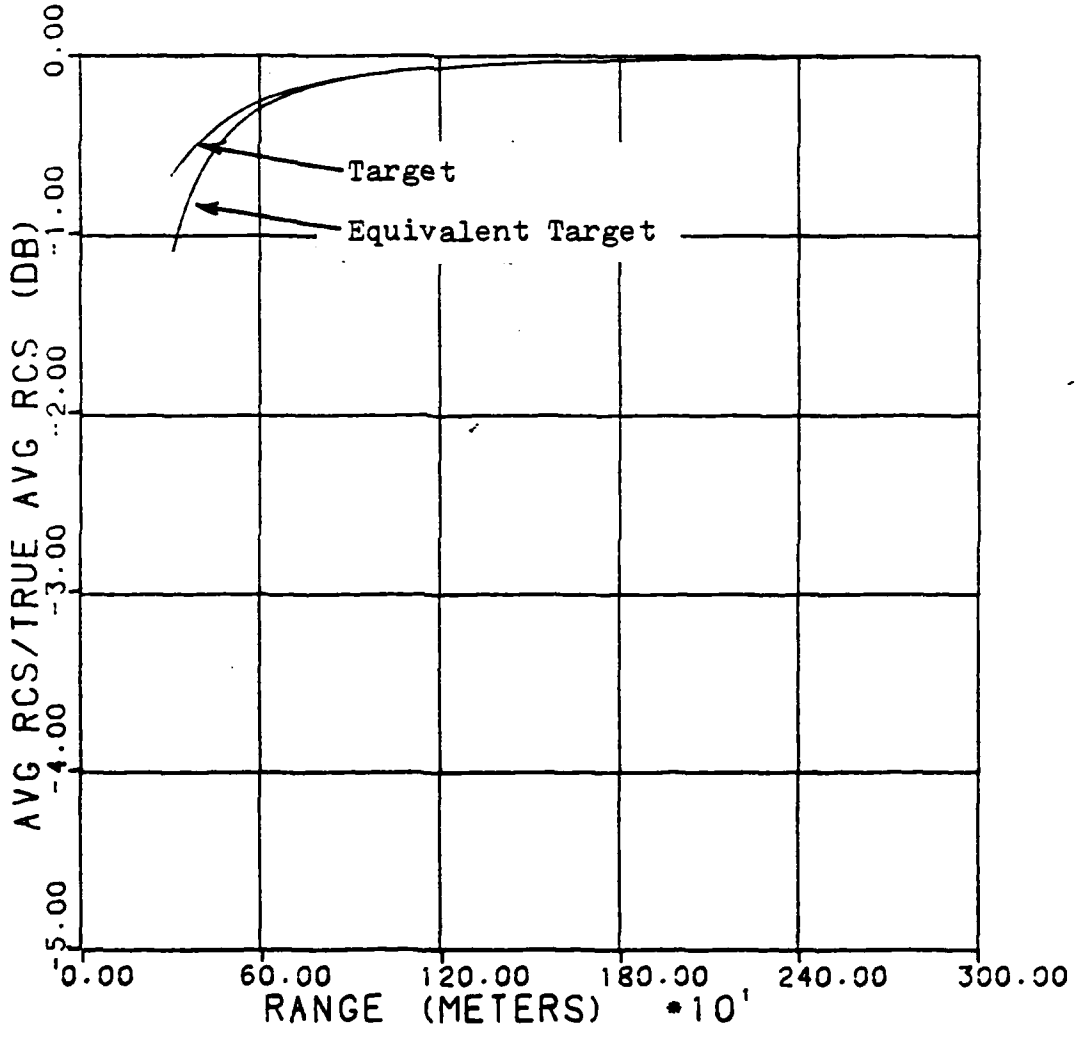

Fig. VIII-10. Comparison of Average RCS Variation for a Specific Target and it's Equivalent Length Target(Target Distribution-$p_a(y)$, $x=3/4$, $L=9.144m$, $W=.9144m$; Equivalent Target-$L'_a=4.88m$; $\theta_3=1.18$ deg)

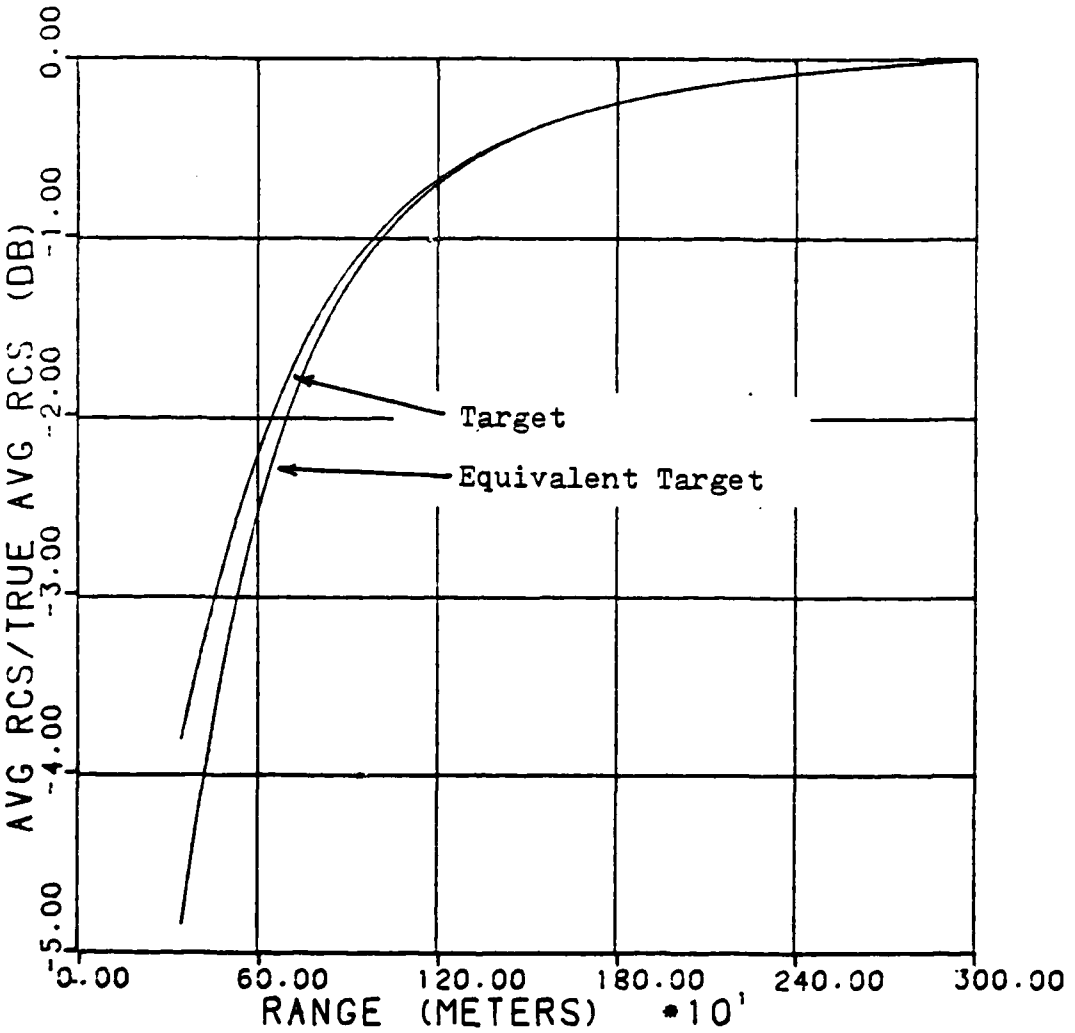

Fig. VIII-11. Comparison of Average RCS Variation for a Specific Target and it's Equivalent Length Target(Target Distribution-$p_b(y)$, m=3, L=18.28m, W=1.828m; Equivalent Target-L_b'=16.7m; θ_3=1.18 deg)

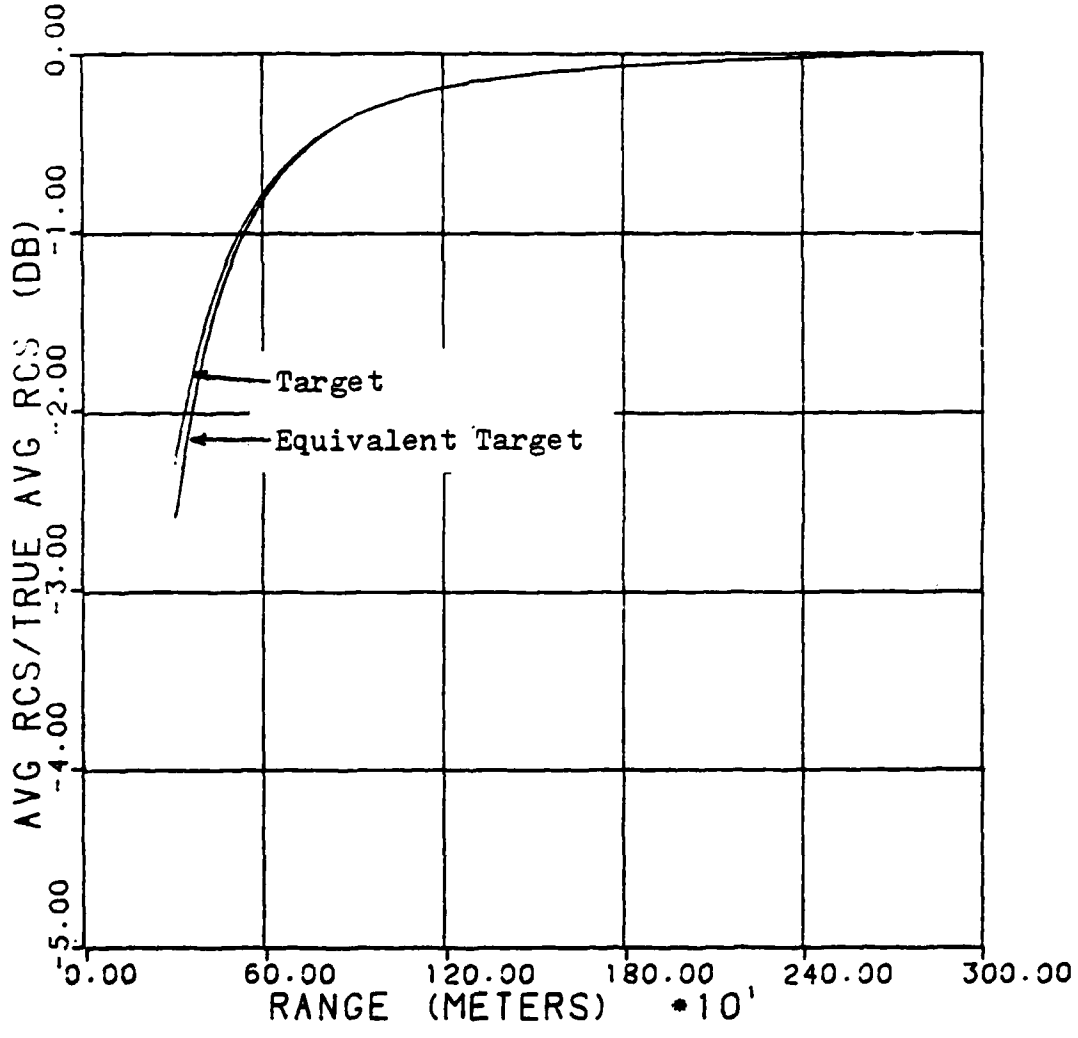

Fig. VIII-12. Comparison of Average RCS Variation for a Specific Target and it's Equivalent Length Target(Target Distribution-$p_b(y)$, m=3 L=9.144m, W=.9144m; Equivalent Target- L_b'=8.36m; θ_3=1.18 deg)

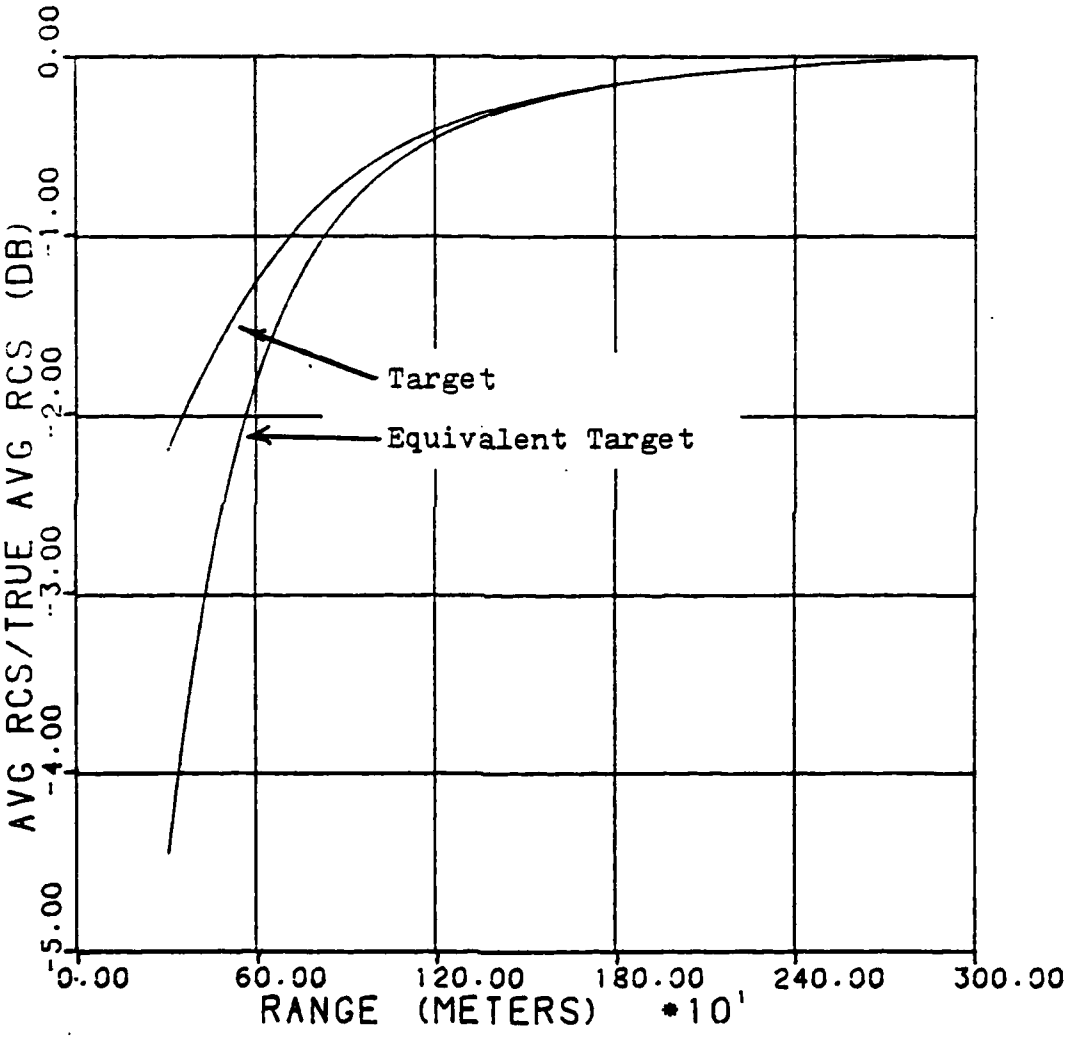

Fig. VIII-13. Comparison of Average RCS Variation for a Specific Target and it's Equivalent Length Target(Target Distribution-$p_b(y)$, m=10, L=18.28m, W=1.828m; Equivalent Target-L_b'=13.32m; θ_3=1.18 deg)

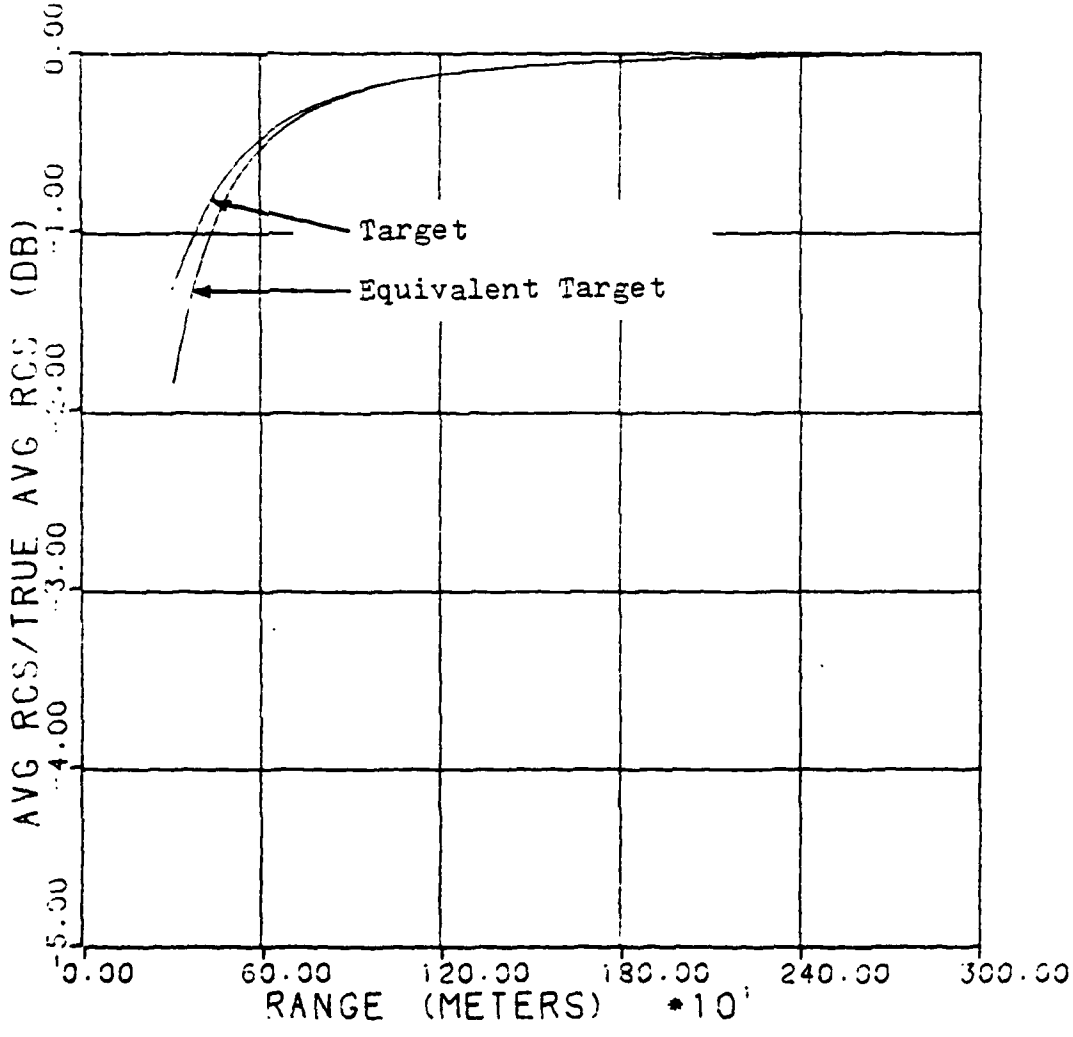

Fig. VIII-14. Comparison of Average RCS Variation for a Specific Target and it's Equivalent Length Target(Target Distribution-$p_b(y)$, m=10, L=9.144m, W=.9144m; Equivalent Target-L_b'=6.66m; θ_3=1.18 deg)

the range is decreased to the point that $(R_m\theta_3)/L' < 1.665$. The fact that Eqs (VIII-11a) and (VIII-11b) are not accurate for values of $R_m\theta_3/L' < 1.665$ suggests that Figure VIII-2 is not applicable, using the equivalent length model, for values of $R_m\theta_3/L' < 1.665$. However, it should be noted that when the parameters of the density functions $p_a(y)$ and $p_b(y)$ meet these restrictions,

$$\frac{W}{L} < x \qquad (p_a(y)) \qquad \text{(VIII-12a)}$$

$$m > 1 \qquad (p_b(y)) \qquad \text{(VIII-12b)}$$

figure VIII-2 shows a worst case situation. The restrictions in Eqs (VIII-12a) and (VIII-12b) cause the height of the density functions [$p_a(y)$ and $p_b(y)$] to be greater in the center than over the outer regions and also causes $L' < L$. When $L' < L$ and the density functions are larger in the center region than over the outer regions

$$\int_{-L/2}^{L/2} \exp\left[\frac{-8\ln 2y^2}{\theta_3^2 R_m^2}\right] p_{a,b}(y)dy \geq \int_{-L'/2}^{L'/2} \exp\left[\frac{-8\ln 2y^2}{\theta_3^2 R_m^2}\right] \frac{1}{L'}dy$$

$$\left[\frac{\bar{\sigma}_m}{\sigma_o}\right]_{a,b} \geq \left[\frac{\bar{\sigma}_m}{\sigma_o}\right]_{L'} \qquad \text{(VIII-13)}$$

Eq (VII-13) means that the equivalent length target will always predict an RCS loss greater than the true RCS loss given by the specific target. Thus Figure VIII-2 can be used safely due to the fact that the curve is a worst case approximation of the RCS loss (when m > 1 and W/L < x).

For cases of m < 1 and W/L > x, the equivalent length is greater than L. For this case, Figure VIII-2 cannot be used accurately for values of $R_m\theta_3/L < 1.665$, since the curve will not necessarily give the worst case approximation.

Truncated Gaussian Distributed Target

The last target model considered is the truncated Gaussian distribution as shown in Figure VIII-15. The standard deviation (SD) is the only parameter of the truncated Gaussian density function.

Using Eq (VIII-5), the normalized average RCS is equal to

$$\left[\frac{\bar{\sigma}_m}{\bar{\sigma}_o}\right]_G = \frac{\operatorname{erf}\left\{\frac{L}{\sqrt{2}}\sqrt{\frac{8\ln 2}{\theta_3^2 R_m^2} + \frac{1}{2(SD)^2}}\right\}}{\operatorname{erf}\left(\frac{L}{2(SD)}\right)\sqrt{\frac{16\ln 2(SD)^2}{\theta_3^2 R_m^2} + 1}} \qquad \text{(VIII-14)}$$

A comparison of results from Eq (VIII-14) and the Monte-Carlo method can be made. Figure VIII-16 shows the typical agreement of the two methods for a specific target.

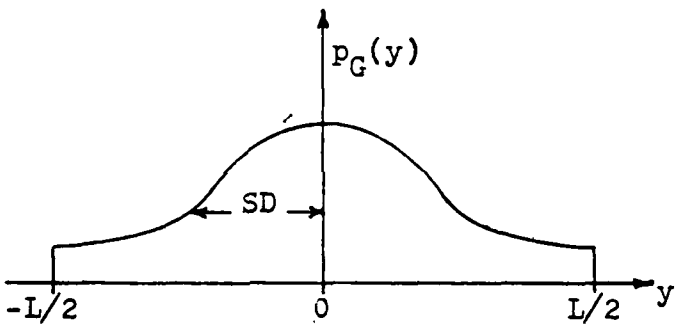

Fig. VIII-15. Gaussian Density of the Point Scatterers Along the Target Length

AD-A138 230 A MINIMUM RANGE CRITERION FOR RCS (RADAR CROSS-SECTION) 2/2
MEASUREMENTS OF A..(U) AIR FORCE INST OF TECH
WRIGHT-PATTERSON AFB OH SCHOOL OF ENGI.. B M WELSH
UNCLASSIFIED DEC 83 AFIT/GE/EE/83D-71 F/G 17/9 NL

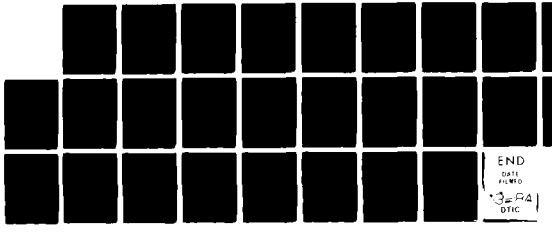

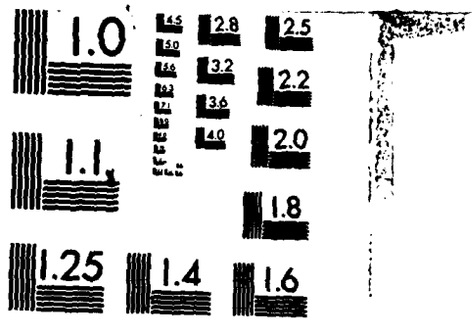

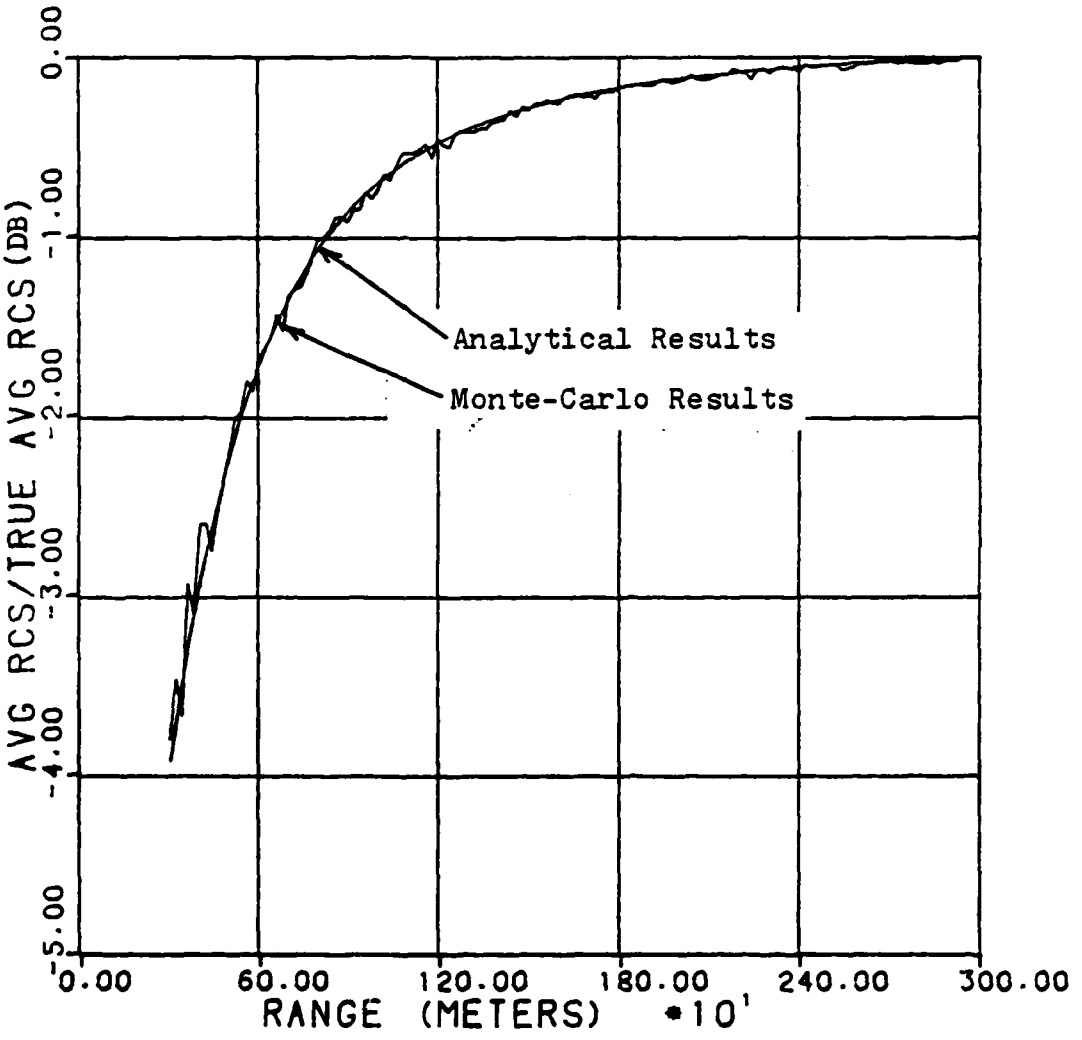

Fig. VIII-16. Average Measured RCS Normalized by the True Average RCS versus Range for a Gaussian Distribution($p_G(y)$, L=18.28m, SD=4.57m, θ_3=1.18 deg)

Again we want to derive an equivalent length target for the truncated Gaussian target. Using Eq (VIII-10) results in the equivalent length

$$L_G' = \sqrt{12}\left\{SD^2 - \frac{L(SD)\exp\left[\frac{-L^2}{8(SD)^2}\right]}{2\sqrt{2\pi}\,\mathrm{erf}\left[\frac{L}{2(SD)}\right]}\right\}^{\frac{1}{2}} \qquad \text{(VIII-15)}$$

Eq (VIII-15) is plotted in Figure VIII-17. Notice that as the standard deviation of the Gaussian distribution decreases, the equivalent length also decreases. Once a target is characterized by a Gaussian distribution, an equivalent length target can be obtained from Eq (VIII-15) and Figure VIII-2 can be used to relate $\overline{\sigma_m}/\overline{\sigma_o}$ to the normalized range. Figures VIII-18 through VIII-21 show some comparisons of the RCS loss curves for the Gaussian target and its equivalent length target. It should be noted that $p_G(y)$ is always larger in the center than on the ends, causing $L_G' < L$. Thus

$$\left[\frac{\overline{\sigma_m}}{\overline{\sigma_o}}\right]_G \geq \left[\frac{\overline{\sigma_m}}{\overline{\sigma_o}}\right]_{L'}$$

and Figure VIII-2 always predicts the worst case approximation of the RCS loss.

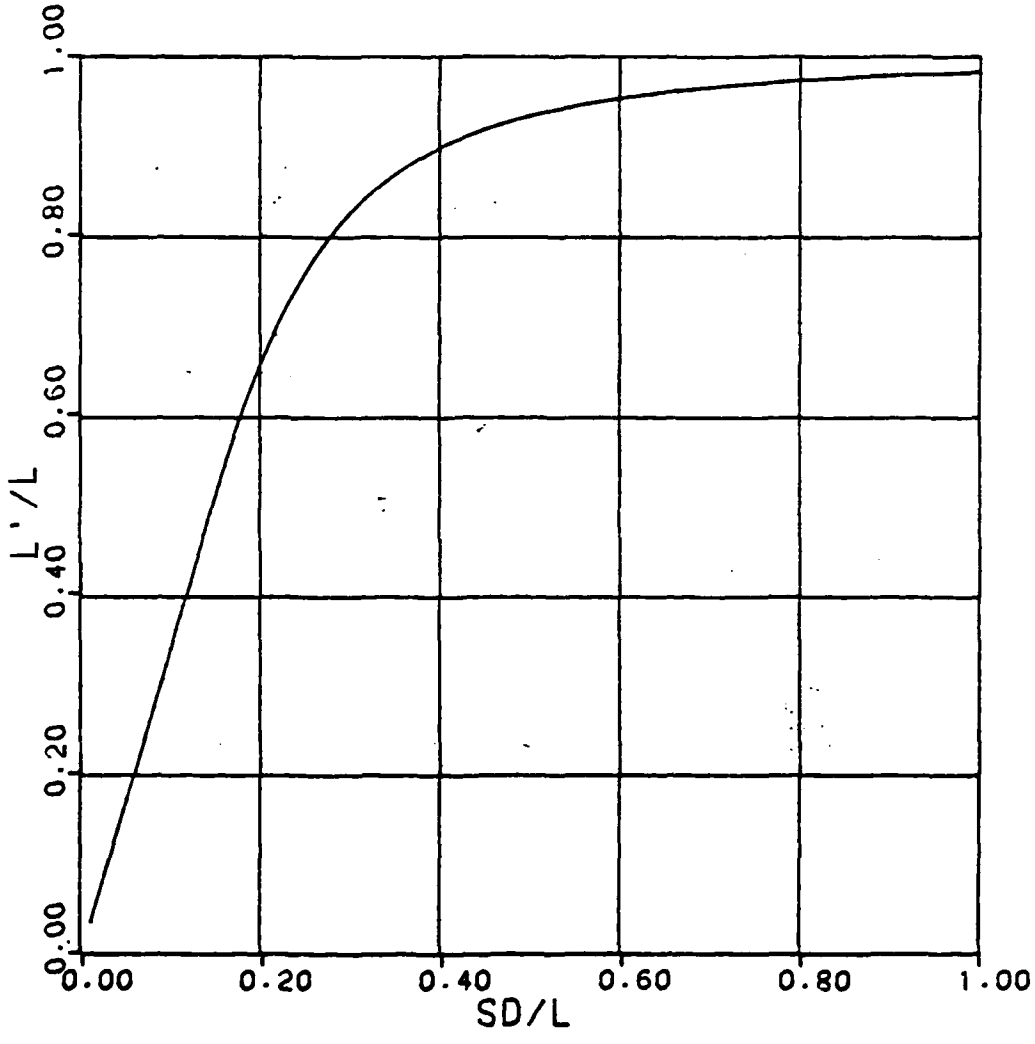

Fig. VIII-17. L'_G/L versus SD/L

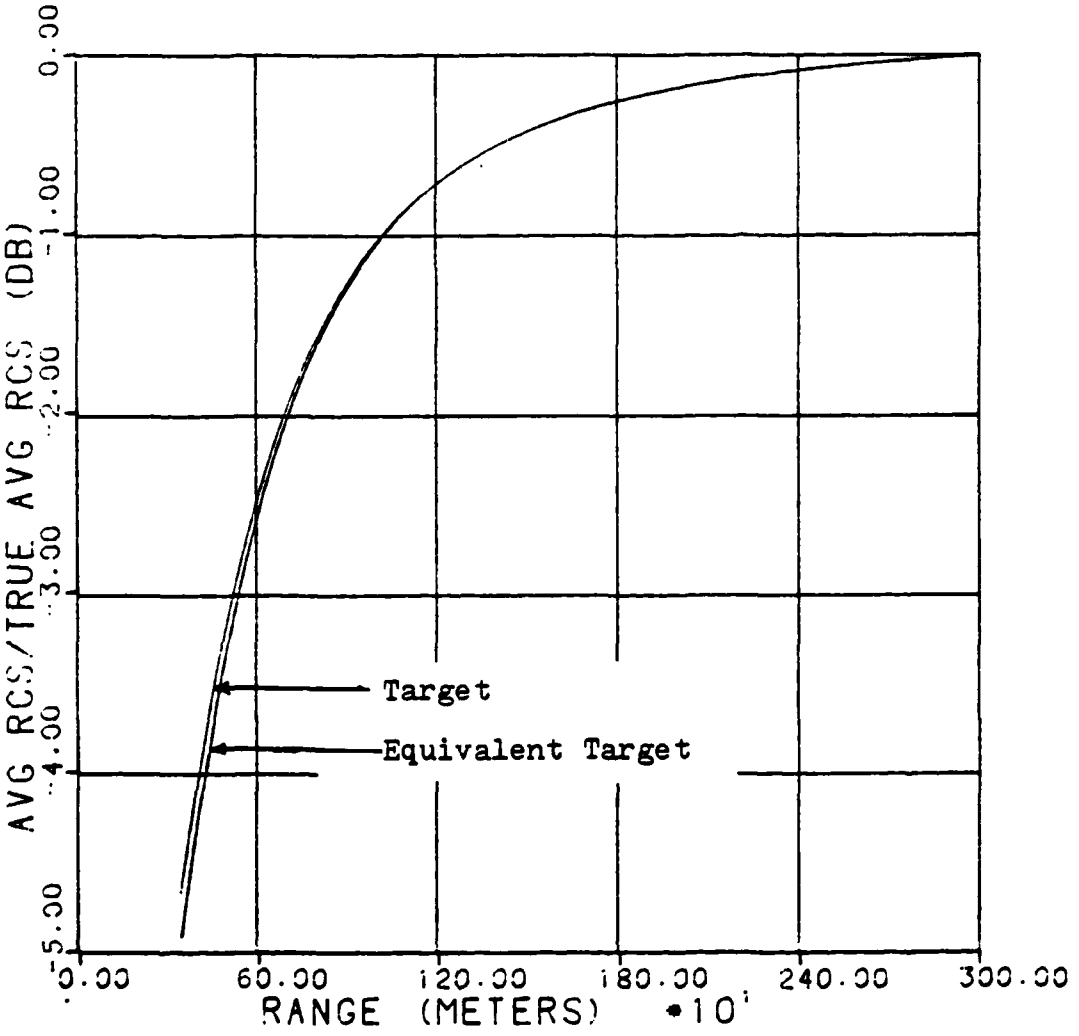

Fig. VIII-18. Comparison of Average RCS Variation for a Specific Target and it's Equivalent Length Target(Target Distribution-$p_G(y)$, SD=9.14m, L=18.28m; Equivalent Target-L'_G=17.0m; θ_3=1.18 deg)

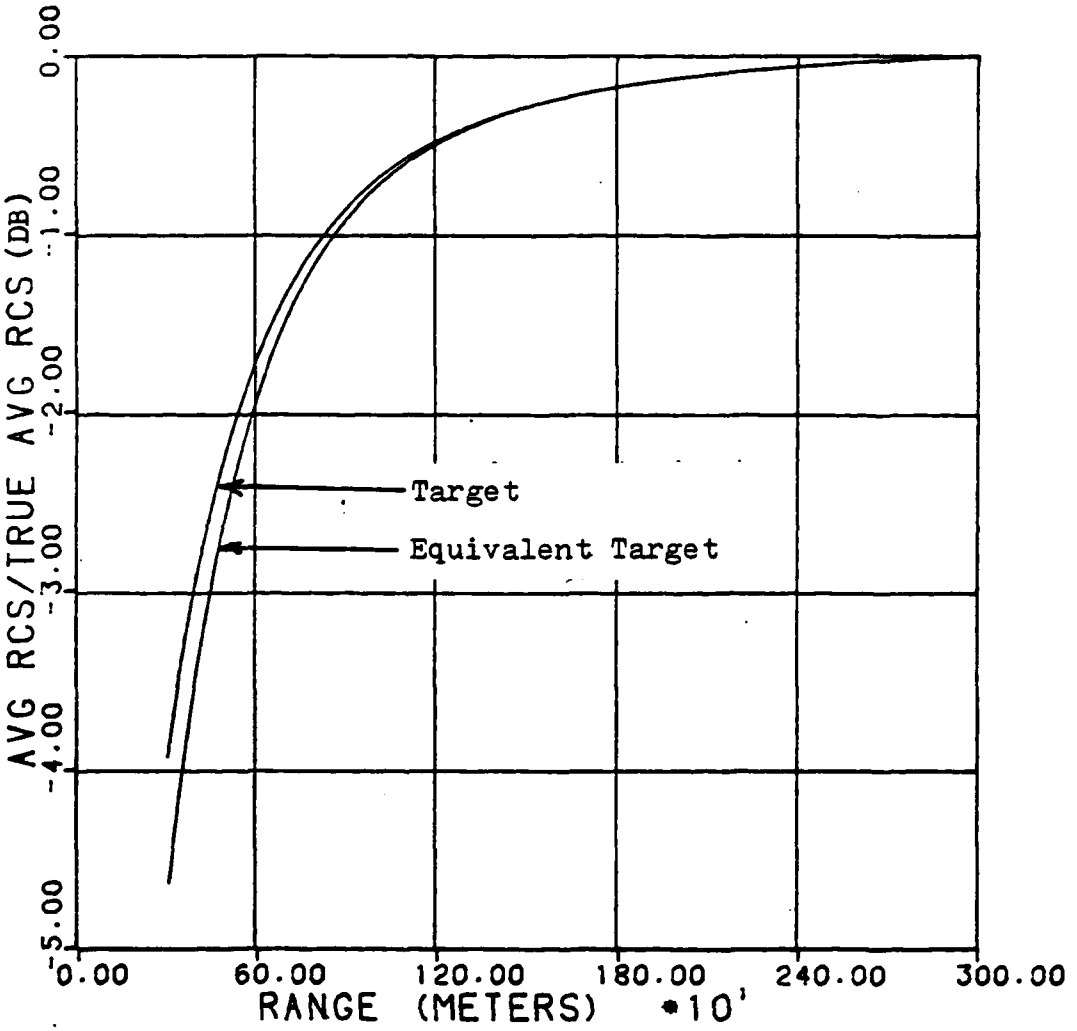

Fig. VIII-19. Comparison of Average RCS Variation for a Specific Target and it's Equivalent Length Target(Target Distribution-$p_G(\dot{y})$, SD=4.57m, L=18.28m; Equivalent Target-L_G'=14.0m; θ_3=1.18 deg)

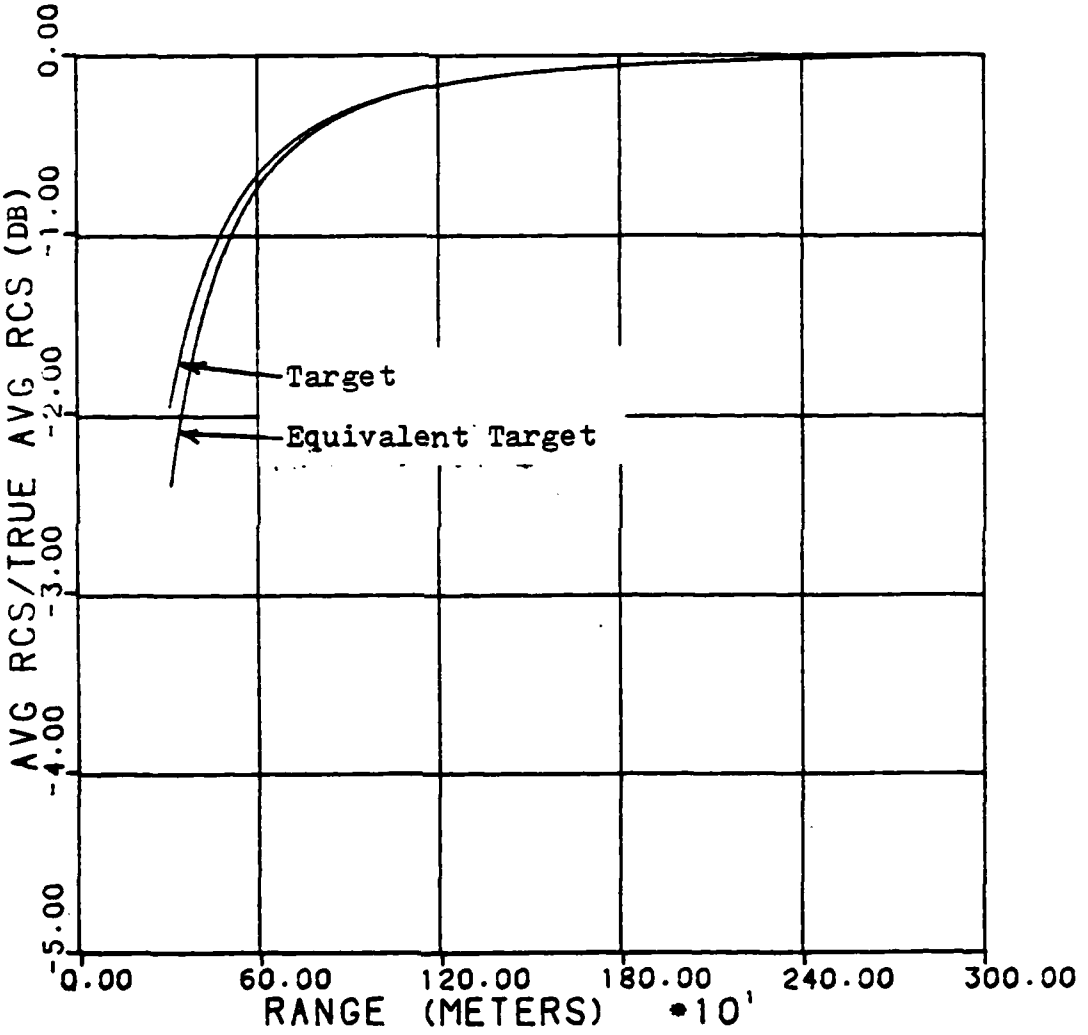

Fig. VIII-20. Comparison Average RCS Variation for a Specific Target and it's Equivalent Length Target(Target Distribution-$p_G(y)$, SD=2.29m, L=18.28m; Equivalent Target-L_G'=7.31m; θ_3=1.18 deg)

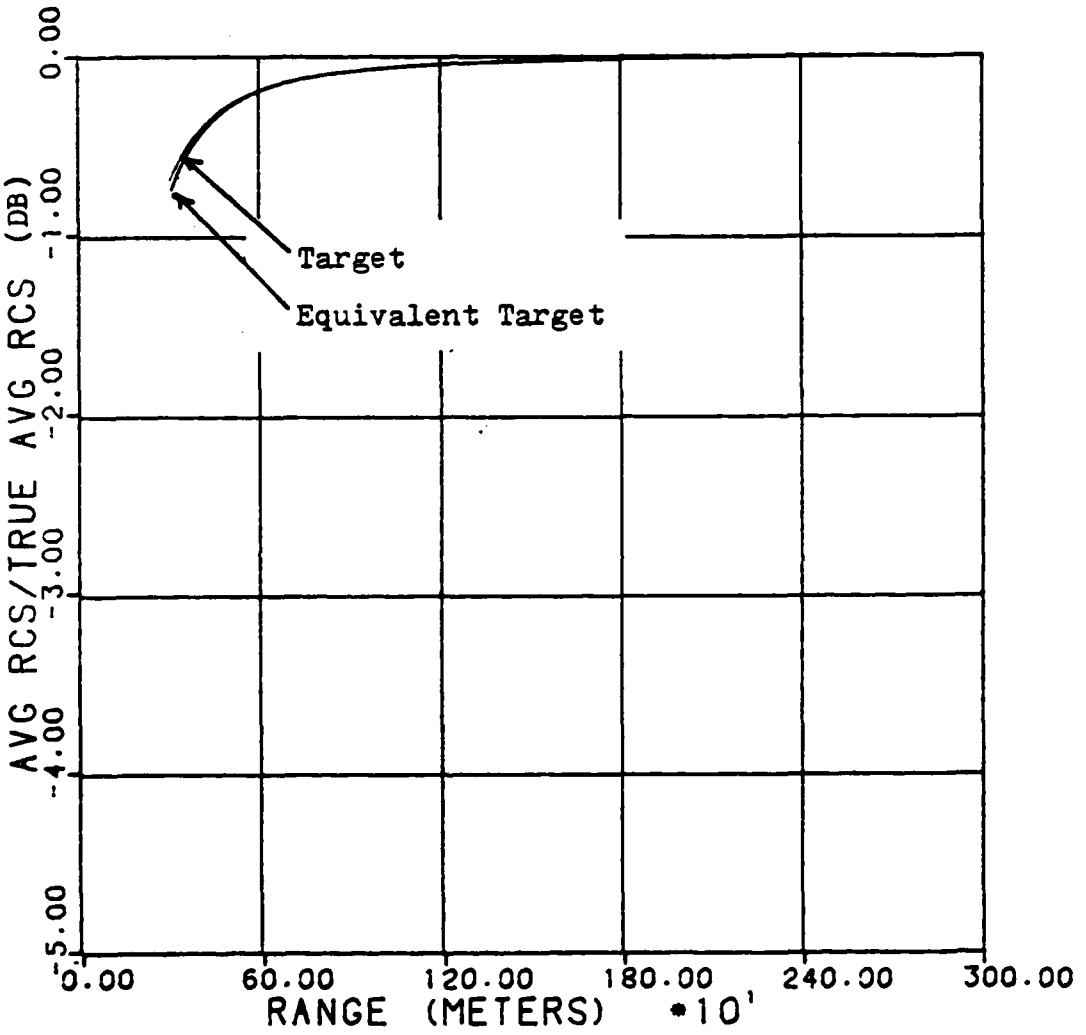

Fig. VIII-21. Comparison of Average RCS Variation for a Specific Target and it's Equivalent Length Target(Target Distribution-$p_G(y)$, SD=1.14m, L=18.28m; Equivalent Target-L_G'=4.2m; θ_3=1.18 deg)

Summary

The dependence of the measured RCS on range, length of target and 3 db beamwidth is examined for each of several target models. For the targets characterized by the stepped uniform and truncated Gaussian spatial distributions, an equivalent length target, characterized by a uniform spatial distribution, is derived. The equivalent length target gives an RCS dependence on range and 3 db beamwidth that approximates the true RCS dependence. Once an equivalent length target is obtained from Eqs (VIII-11) and (VIII-15), Figure VIII-2 can be used to find the minimum range that will result in a specific measured RCS error.

IX. The 3 db Beamwidth of the Antenna Pattern in the Vertical Plane

Introduction

In the previous chapters, the target model is assumed to be lying horizontal to the ground. Due to the horizontal orientation of the target, the 3 db beamwidth is only calculated for a horizontal cut of the antenna pattern. Normally RCS measurements of typical targets are made such that the long dimension of the target is horizontal to the ground, but cases will arise that the long dimension of the target is vertically oriented.

The target models of Chapter V are again used to model the vertically oriented point scattering targets. The only difference in this situation is that the target model is oriented perpendicular to the ground and the center of the model is located at the maximum of the vertical antenna pattern. Finding the minimum measurement range is performed exactly as in the case of the horizontal target model. Figure VIII-2 is again used to obtain the minimum range criterion, but a different method of calculating the 3 db beamwidth must be developed.

3 db Beamwidth

The 3 db beamwidth in the horizontal dimension is given simply by Figure VII-3; however, the 3 db beamwidth in the

vertical dimension is quite complicated to calculate analytically. The approach used in this thesis is to find the 3 db beamwidth numerically.

The parameters that affect the 3 db beamwidth are the aperture illumination pedestal height (C), tilt angle (θ_T), height of the antenna above the ground (D), wavelength (λ) and the radius of the parabolic dish (a). The graphs in Figures IX-2 through IX-4 show the 3 db beamwidth relative to these antenna parameters.

Before discussing the graphs, a point must be discussed. The main lobe of the vertical antenna pattern is assumed to be approximately Gaussian shaped. The minimum range criterion developed in this thesis depends on the validity of this Gaussian approximation. The main lobe of the vertical antenna pattern is not always well approximated by the Gaussian shape. For certain parameter combinations, the first null of the image antenna pattern is within the 2 db beamwidth of the main lobe of the source antenna pattern. When the two antenna patterns are added together to form the total pattern, the null of the image pattern distorts the main lobe of the total antenna pattern. Figure IX-1 shows the distortion caused by the null of the image pattern. The distorted antenna pattern is not well approximated by the Gaussian shape and is not considered in the 3 db beamwidth graphs (Figures IX-2 to IX-4).

Figure IX-2 illustrates the regions that the Gaussian shape is a good approximation to the main lobe of the antenna

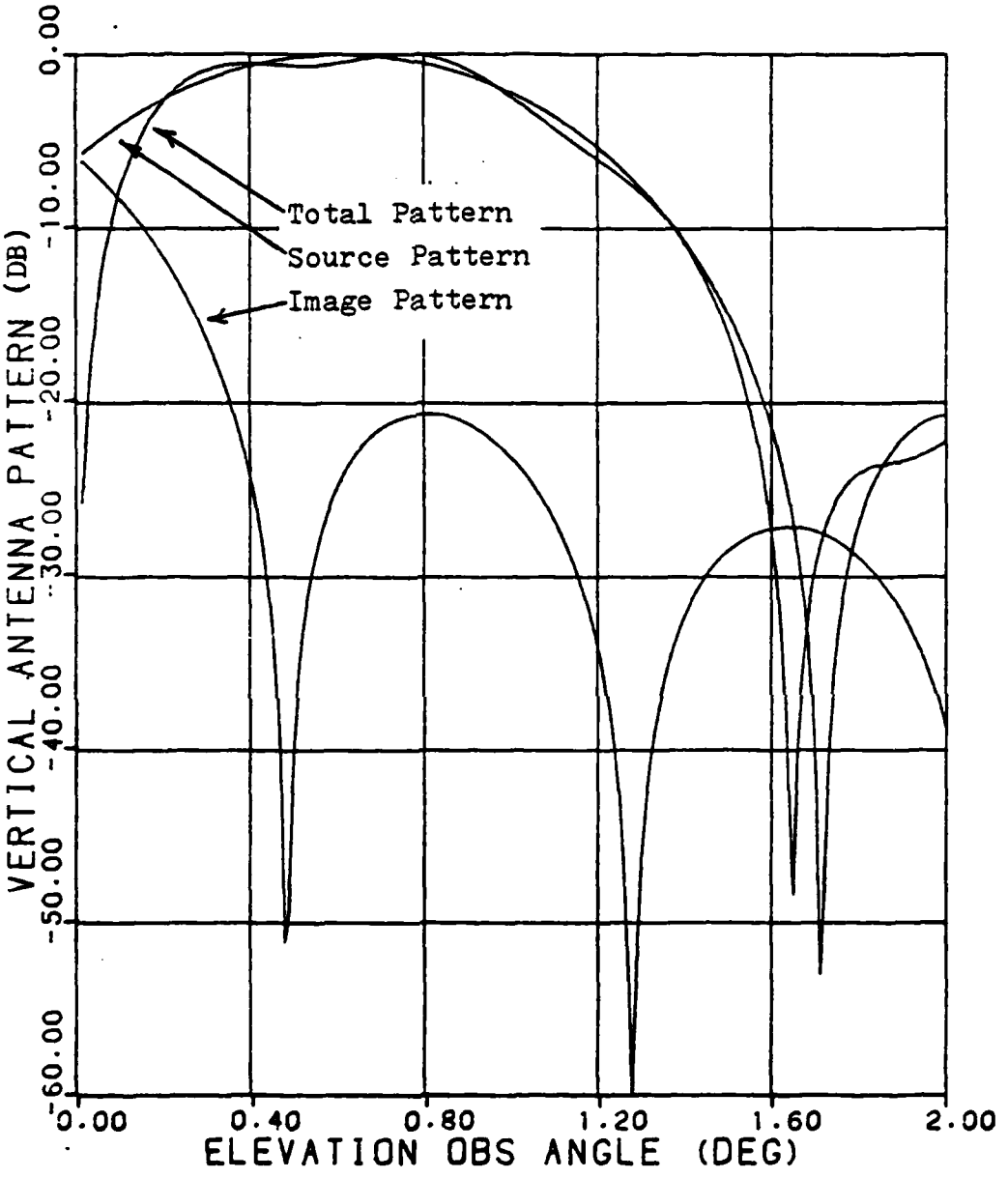

Fig. IX-1. Distortion of the Antenna Pattern caused by Image Pattern Null

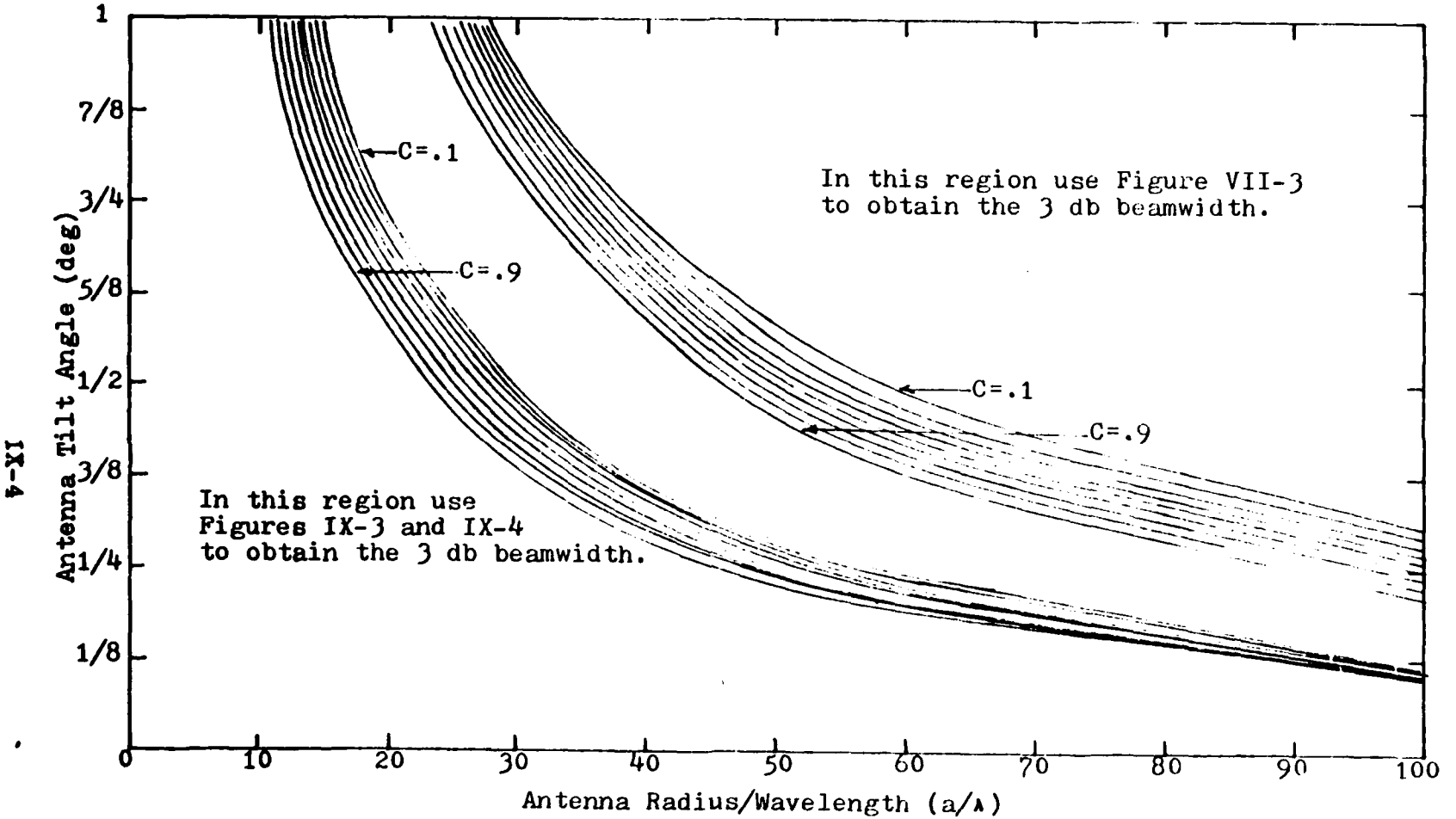

Fig. IX-2. Graph of Separate Operating Regions for Ground Bounce Antenna Pattern

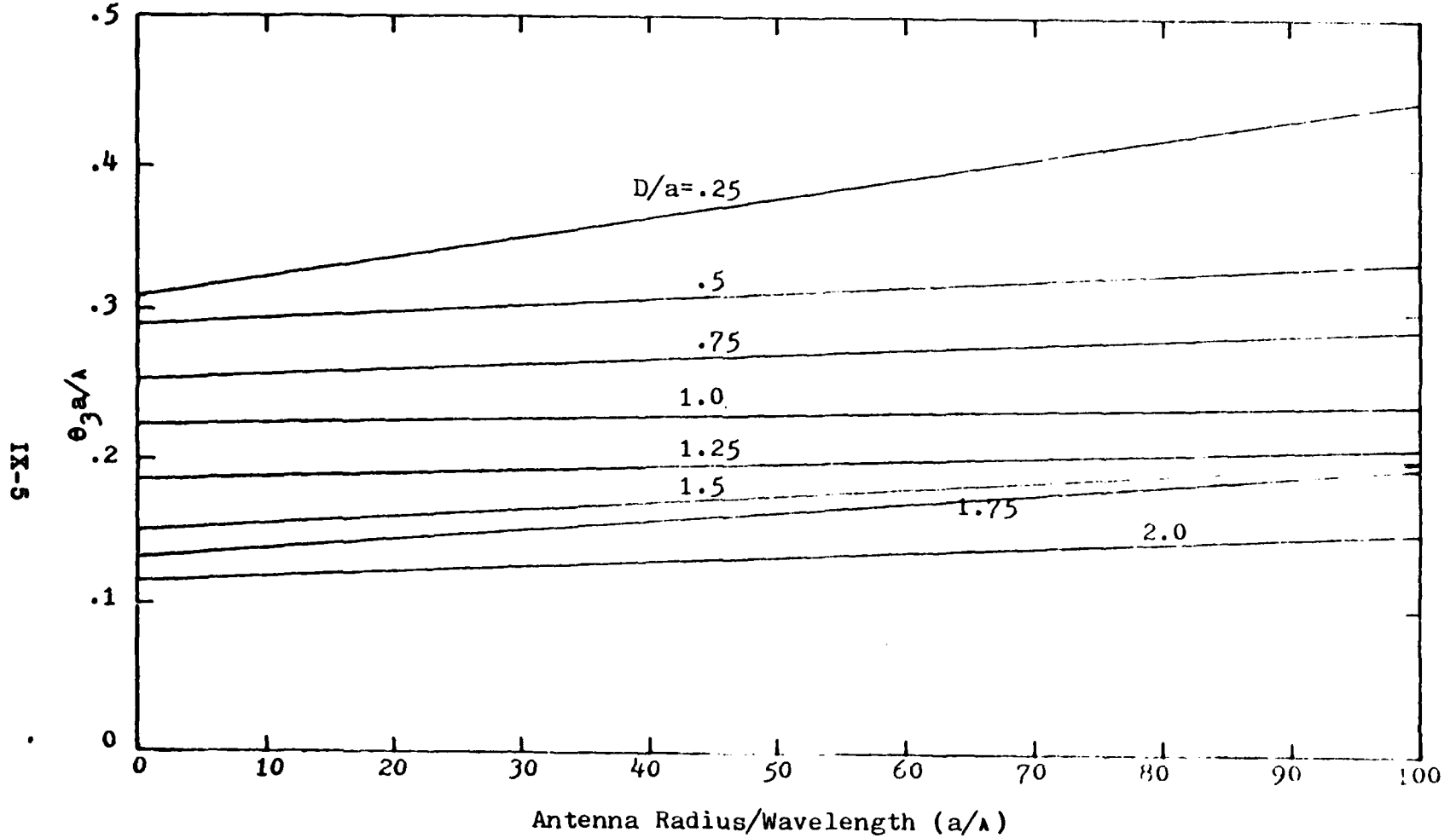

Fig. IX-3. Normalized 3 db Beamwidth versus a/λ ,(C=.5)

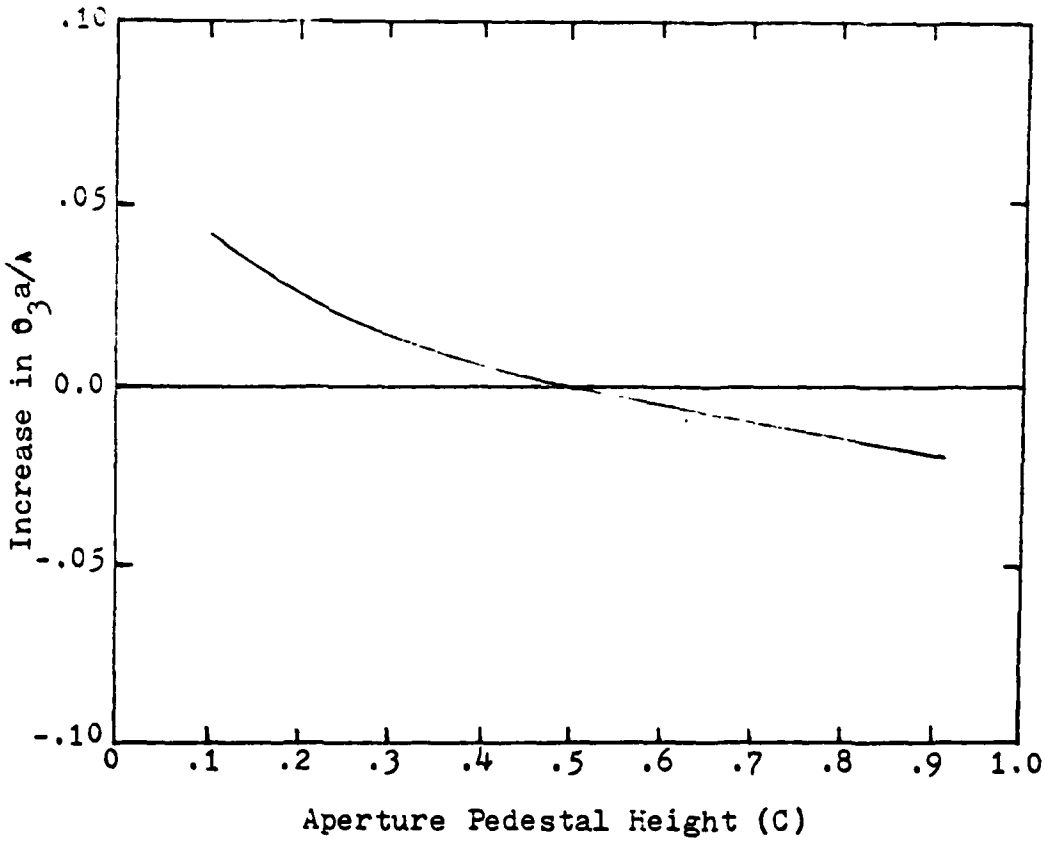

Fig. IX-4. Graph of Correction added to Result of Figure IX-3 for values of C other than .5

pattern. If the parameters of the antenna pattern are such that the operating point is above the upper curve (for a particular C) in Figure IX-2, the 3 db beamwidth is roughly estimated by Figure VII-3. The accuracy of Figure VII-3 improves as the operating point is moved further away from the upper curve. If the operating point is between the upper and lower curves of Figure IX-2, the antenna pattern is *not* well approximated by the Gaussian shape. If the operating point is below the lower curve, Figures IX-3 and IX-4 must be referenced. Figure IX-3 shows the normalized 3 db beamwidth versus a/λ for $C = .5$. For other values of C, Figure IX-4 gives a correction term to add to the result from Figure IX-3.

X. Conclusions

A minimum range criterion has been developed for RCS measurements of those targets dominated by point scatterers and of such a size that only average RCS data is required. The target dominated by point scatterers was not examined in the traditional approach outlined in Chapter II. The traditional approach only considered the target characterized by flat surfaces and developed a minimum range criterion based on the maximum allowable amplitude and phase variation of the incident field across the target. The traditional minimum range criterion is shown in Eq (II-2) for the source modeled as a point source, and Figure II-4 for the source modeled as a square aperture.

Approach to Obtaining the New Minimum Range Criterion

The steps taken to develop a minimum range criterion for the point scattering target were

(1) modeling the RCS measurement range

(2) modeling the target probabilistically

(3) obtaining an analytical and Monte-Carlo method for finding the statistics of the measured RCS relative to the statistics of the "true" RCS

(4) relating the results of Step (3) for several target models to a baseline model and using this baseline model to obtain a minimum range criterion.

Step (1) modeled a ground bounce RCS measurement range. The measurement range was characterized by a parabolic reflector dish antenna. The ground bounce characteristic was modeled by effectively removing the ground and placing the antenna's image below the ground level. Chapter IV detailed the development of the measurement range model.

Step (2) involved defining several target models to be used. The targets consisted of a statistical distribution of point scatterers of equal magnitude along a straight line of length L. The spatial distributions used were a uniform, a stepped uniform and a Gaussian distribution. The target characterized by the uniform distribution was the baseline for comparisons of the other targets.

Step (3) consisted of developing an analytical approach to solving for the measured RCS of the target and validating this by a numerical experiment using a Monte-Carlo simulation. From Chapter VI the measured RCS was found to be proportional to $E[F^4(\theta,\phi)]$, where $F(\theta,\phi)$ was the normalized antenna pattern. The variables θ and ϕ were random variables related to the random position of the scatterers on the target. Only the relative changes of the measured RCS dependent on range were needed. The Monte-Carlo simulation used the measurement range model and the target models to obtain $E[F^4(\theta,\phi)]$. A computer was used to generate the antenna pattern from the model given in Chapter IV and a random number generator was used to simulate the random position of the scatterers along the target

length. Many numerical experiments were averaged, as shown in Eq (VII-7), to give an approximation of $E[F^4(\theta,\emptyset)]$.

The analytical approach involved approximating the main lobe of the antenna pattern, at the target, by a Gaussian shape. The Gaussian shape was a very good approximation to the real antenna pattern near the center of the main beam and was also mathematically simple to work with. As a result of the Gaussian antenna pattern approximation, $E[F^4(\theta,\emptyset)]$ was expressed in terms of error functions. The results from the analytical approach were verified by comparing them to the results from the Monte-Carlo approach.

Step (4) derived an expression that related the targets characterized by the stepped and Gaussian spatial distributions to the target characterized by the uniform spatial distribution. An "equivalent length" target was developed. The equivalent length target had a length L' and was characterized by the uniform spatial distribution of the point scatterers. The normalized RCS versus range data for a stepped uniform or Gaussian target was approximated by its equivalent length target. The expressions for the equivalent length targets were shown in Eqs (VIII-11) and (VIII-15).

A minimum range criterion was obtained from the uniform target model. The minimum range criterion was given in the form of a graph of RCS loss versus normalized range. This graph is shown in Figure VIII-2. The RCS loss shown on the vertical axis was the reduction which the average of the

measured RCS would experience, relative to the average of the true RCS due to range considerations.

Examples

Some examples compare the traditional minimum range criteria to the range criterion shown in Figure VIII-2. Consider a target dominated by point scatterers having a length of 18.28m (60 ft). Assume the scattering points are uniformly distributed along the length of the target. The measurement antenna is a parabolic reflector dish of diameter 1.828m (6 ft), operating at 9.6 GHz (assume an aperture illumination pedestal height, C, of .1). From Figure VII-3, the 3 db beamwidth of the horizontal antenna pattern is 1.18°. Also assume that an RCS measurement error of 1 db can be tolerated. The minimum allowable measurement range can be obtained from Figure VIII-2. The minimum measurement range is 1.2 km.

In the traditional approach, Kouyoumjian and Peters state that 1 db of RCS measurement error can be expected if the incident field at the target has a phase variation of $\pi/8$ radians and an amplitude variation of 1 db over the extent of the target. Allowing a phase variation of $\pi/8$ radians in the traditional range criterion for the point source antenna results in

$$R_m = \frac{2L^2}{\lambda} \qquad \text{(X-1)}$$

The minimum range obtained from Eq (X-1), for the example at hand, is $R_m = 2(18.28)^2/(.03125) = \underline{21.4 \text{ km}}$.

The traditional minimum range criterion for the square aperture is shown in Figure II-4. For an aperture of comparable size to the parabolic dish ($\ell = 2a = 1.828$m), ℓ/L is equal to .1. The minimum range obtained from Figure II-4, considering only the maximum allowable amplitude variation across the target, is approximately 2.1 km. The minimum range from Figure II-4, considering only phase variation, is the same as the result of point source antenna, 21.4 km.

The rough minimum range criterion developed by Hendrick (Chapter III) is shown in Table III-1. For the example at hand, L/λ is much greater than 50 , resulting in the use of

$$R_m = \frac{L^2}{4\lambda}$$

and a minimum measurement range of 2.6 km.

As seen from the example, when the maximum phase variation across the target is limited to $\pi/8$ radians, the traditional minimum range criterion is vastly larger than necessary. If only the amplitude variation across the target is considered, for the square aperture antenna, the minimum range is slightly larger than the range predicted by Figure VIII-2. Hendrick's minimum range criterion also gives a slightly larger minimum range than the minimum range given by Figure VIII-2. These last two minimum range criteria give similar results to the minimum range criterion shown in Figure VIII-2, because all

three are based only on the amplitude variation of the incident field.

As another example, consider the target having all of the diffracting points concentrated at each end of the target's length. Using the stepped distribution $p_a(y)$ in Figure VIII-3 to describe the target, the equivalent length for the target is

$$L'_a = L\sqrt{\frac{(\frac{W}{L})^2(x-\frac{W}{L}) + (1-x)}{1 - \frac{W}{L}}}$$

where x = 0 and W approaches L.

$$L'_a = \lim_{W \to L} \; L\sqrt{\frac{1 - (\frac{W}{L})^3}{1 - (\frac{W}{L})}}$$

$$= \sqrt{3}L$$

Using the same length target as in the first example, 18.28m (60 ft), the equivalent length is 31.669 m (103.9 ft). Again using an antenna beamwidth of 1.18°, and an acceptable RCS loss of 1 db, the minimum range obtained from Figure VIII-2 is 2.08 km. Recall that the RCS loss given by Figure VIII-2 is not a worst case prediction of the true loss for the cases of W/L > x (see Chapter VIII). This may cause the minimum range to be too short. Going back to Eq (VII-6) and calculating the minimum range for the target being considered, the correct minimum range is 2.18 km.

The traditional minimum range criterion and Hendrick's minimum range criterion give the same minimum ranges as in the first example. Again, the traditional minimum range criterion, when phase variation is considered, is vastly larger than required. The minimum range for the square aperture antenna, when amplitude variation is considered, is almost equal to the range given by Figure VIII-2. Hendrick's minimum range is also close to the range given by Figure VIII-2.

As seen from both examples, the minimum range criterion developed in this thesis is dependent on how the positions of the scatterers are characterized as well as the length of the target, for a given frequency and antenna. However, the traditional minimum range criterion and Hendrick's minimum range criterion depend only on the target length, for a given frequency and antenna. The new minimum range criterion is sensitive to target characteristics, and gives a minimum measurement range that reflects these characteristics.

Steps to Use the New Minimum Range Criterion

Outlined below are the steps taken to obtain the minimum measurement range for the target dominated by point scatterers.

(1) characterize the target's spatial distribution of scattering points as

(a) uniform

(b) stepped uniform

(c) truncated Gaussian

(d) other

(2) find the equivalent length target corresponding to the specific target by using Eq (VIII-11) or (VIII-15)

(3) determine the 3 db beamwidth of the measurement antenna pattern either by using Figure VII-3 and Figures IX-2 through IV-4 for a parabolic dish, or by some other suitable means

(4) use Figure VIII-2 to obtain the minimum range necessary for a given RCS loss or use Eq (VII-6) for target distributions not considered in this thesis.

Some Generalizations

In this thesis, the main lobe of the antenna pattern was assumed to be approximated accurately by a Gaussian shape. This assumption may not always be valid. The Gaussian shape was used due to its mathematical simplicity and its good agreement with the antenna pattern developed in Chapter IV. Other approximations of the antenna pattern can certainly be used for the analytical approach outlined in Chapter VII. All that is required is to replace the Gaussian expression in Eq (VII-6) by the appropriate approximation.

If the case arises that an approximation is not easily found and only measurements of the pattern are available, then the Monte-Carlo method can be used. The Monte-Carlo method is used in this situation by storing the measured antenna pattern data in the computer and retrieving the pattern data for each random scatterer position selected on the target and then performing the averaging of Eq (VII-1).

Bibliography

1. Beckmann, Petr. "Statistical Distribution of the Amplitude and Phase of a Multiply Scattered Field." Journal of Research of the National Bureau of Standards-D. Radio Propagation, Vol. 66D, No. 3: 231-240 (May-June 1962).

2. Cohen, Albert, A. W. Maltese. "The Lincoln Laboratory Antenna Test Range," Microwave Journal: 57-65 (April 1961).

3. Golden, August. Radar Electronic Warfare. Student Report, Maxwell AFB, AL., Air Command and Staff College, ATC, (83-890).

4. Hendrick, Lee R. "Analytical Investigation of Near Zone/Far Zone Criteria," Radar Reflectivity Measurement Symposium. 5-19, Hanscom AFB, Mass.: Rome Air Development Center, July 1964. (RADC-TDR-64-25, AD 601 305).

5. Ishimaru, Akira. Wave Propagation and Scattering in Random Media, Vol. 1. New York: Academic Press, 1978.

6. Kouyoumjian, R. G. "An Analysis of Reflection Measuring Systems," Radar Reflectivity Measurement Symposium. 127-145. Griffis AFB, N.Y.: Space Surveillance and Instrumentations Branch, Rome Air Development Center, April 1964. (RADC-TDR-64-25).

7. Kouyoumjian, R. G., L. Peters. "Range Requirements in Radar Cross Section Measurements," Proceedings of the Institute of Electrical and Electronics Engineers, Vol. 53. 920-928 (Aug. 1965).

8. Papoulis, A. Probability, Random Variables, and Stochastic Processes. New York: McGraw-Hill Book Company, 1965.

9. Ramsey, John F. "Antenna Design Supplement," Microwave Journal, Vol. 6: 69-107 (June 1967).

10. Skolnik, Merrill. Introduction to Radar Systems. New York: McGraw-Hill Book Company, 1980.

11. Stutzman, W. L., Gary A. Thiele. Antenna Theory and Design. New York: John Wiley and Sons, Inc., 1981.

Appendix A

Calculation of the Fields from a Circular Aperture, Assuming an Aperture Field Distribution of a Parabolic Taper on a Pedestal

Aperture integration is used to calculate the fields from the circular aperture of the parabolic dish. Figure A-1 shows the geometry of the problem. For the following calculations, these assumptions are made:

$$2a >> \lambda \tag{A-1}$$

$$\bar{E}_a(\bar{r}') = \hat{x}E_a(\bar{r}') \tag{A-2}$$

where

a is the radius of the circular aperture
$\bar{E}_a(\bar{r}')$ is the aperture field.

The aperture field is expressed

$$E_a(r') = C + (1-C)\left[1 - \left(\frac{r'}{a}\right)^2\right] \tag{A-3}$$

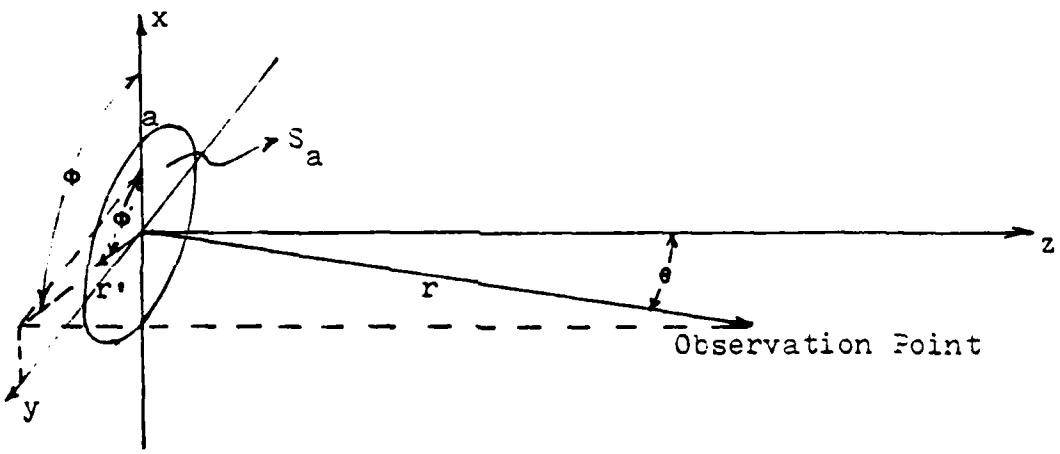

Fig. A-1. Circular Aperture Geometry for a Single Parabolic Reflector Dish

where C is the pedestal height (see Figure A-2). From Stutzman and Thiele (Ref 11:382), the vector $\bar{P}$ is defined as an integral over the aperture area

$$\bar{P} = \iint_{S_a} \bar{E}_a \, e^{j\beta \hat{r} \cdot \bar{r}'} \, ds' \tag{A-4}$$

The electric potential, $\bar{F}$, is defined

$$\bar{F} = \frac{-e^{j\beta r}}{4\pi r}(-P_y \hat{x} + P_x \hat{y}) \tag{A-5}$$

Since $\bar{E}_a$ has only an $\hat{x}$ component

$$P_x = \iint_{S_a} E_{a_x}(r') e^{j\beta(r'\cos\phi'\sin\theta\cos\phi + r'\sin\phi'\sin\theta\sin\phi)} ds'$$

$$P_x = \int_0^{2\pi} \int_0^{a} E_{a_x}(r') e^{j\beta r'\sin\theta\cos(\phi-\phi')} r' dr' d\phi' \tag{A-6}$$

Using the integral identify (Ref 11:566)

$$J_o(x) = \frac{1}{2\pi} \int_0^{2\pi} e^{jx\cos\alpha} d\alpha$$

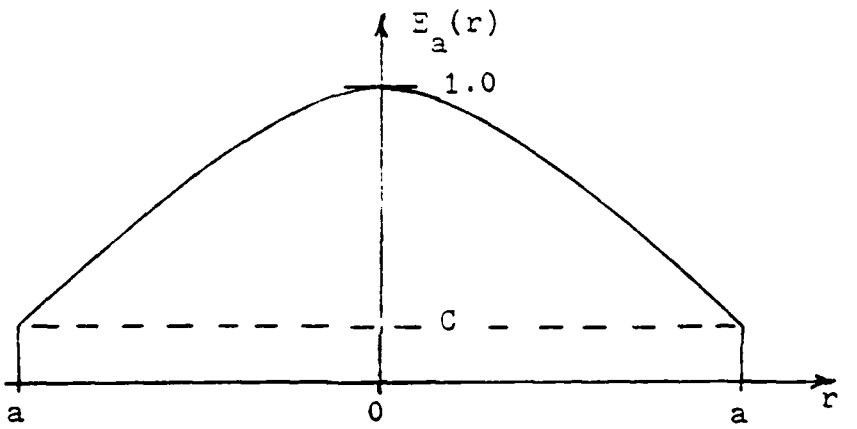

Fig. A-2. Aperture Field Distribution

where $J_o(x)$ is a cylindrical Bessel function, Eq (A-6) can be written

$$P_x = 2\pi \int_0^a E_{a_x}(r') r' J_o(\beta r' \sin\theta) dr' \qquad (A-7)$$

Substituting the aperture distribution [Eq (A-3)] into Eq (A-7) results in

$$P_x = 2\pi \int_0^a \left[C + (1-C)\left[1 - \left(\frac{r'}{a}\right)^2\right]\right] r' J_o(\beta r' \sin\theta) dr'$$

$$= 2\pi \int_0^a C r' J_o(\beta r' \sin\theta) dr' +$$

$$2\pi \int_0^a r'(1-C)\left[1 - \left(\frac{r'}{a}\right)^2\right] J_o(\beta r' \sin\theta) dr'$$

(A-8)

The first integral of Eq (A-8) can be simplified using the integral identity (Ref 11:566)

$$\int_0^1 x^{n+1} J_o(x) dx = x^{n+1} J_{n+1}(x)$$

The second integral can be simplified by using the identity (Ref 11:566)

$$\int_0^1 (1-x^2)^n x J_o(bx) dx = \frac{2^n n!}{b^{n+1}} J_{n+1}(b)$$

The final expression for P_x is

$$P_x = \frac{2\pi aCJ_1(\beta a \sin\theta)}{\beta \sin\theta} + \frac{-\pi(1-C)J_2(\beta a \sin\theta)}{\beta^2 \sin^2\theta} \qquad \text{(A-9)}$$

where $J_1(x)$ and $J_2(x)$ are cylindrical Bessel functions of the first kind of orders 1 and 2.

The electric field can be found by using (Ref 11:383)

$$E_\theta = \frac{j\beta e^{-j\beta r}}{4\pi r}(P_x \cos\phi + P_y \sin\phi) \qquad \text{(A-10)}$$

$$E_\phi = \frac{j\beta e^{-j\beta r}}{2\pi r} \cos\theta(P_y \cos\phi - P_x \sin\phi) \qquad \text{(A-11)}$$

The resulting fields are

$$E_\theta = j\frac{e^{-j\beta r}}{4\pi r}\frac{2\pi}{\sin\theta}\left[aCJ_1(\beta a \sin\theta) + \frac{2(1-C)J_2(\beta a \sin\theta)}{\beta \sin\theta}\right]\cos\phi \qquad \text{(A-12)}$$

$$E_{\phi} = -j\frac{e^{-j\beta r}}{4\pi r}\frac{2\pi\cos\theta}{\sin\theta}\left[aCJ_1(\beta a\sin\theta) + \frac{2(1-C)J_2(\beta a\sin\theta)}{\beta\sin\theta}\right]\sin\phi \quad \text{(A-13)}$$

VITA

Byron M. Welsh was born on 21 January 1960 in Columbus, Mississippi. He graduated from high school in Lexington, Virginia in 1978 and attended the Virginia Military Institute from which he received the degree of Bachelor of Electrical Engineering in May 1982. Upon graduation, he received a commission in the USAF through the ROTC program. Upon starting active duty, he entered the School of Engineering, Air Force Institute of Technology in June 1982.

Permanent address: Rt. 1, Box 527
Lexington, Virginia 24450

UNCLASSIFIED

SECURITY CLASSIFICATION OF THIS PAGE (When Data Entered)

REPORT DOCUMENTATION PAGE		READ INSTRUCTIONS BEFORE COMPLETING FORM
1. REPORT NUMBER AFIT/GE/EE/83D-71	2. GOVT ACCESSION NO. AD-A138 230	3. RECIPIENT'S CATALOG NUMBER
4. TITLE (and Subtitle) A MINIMUM RANGE CRITERION FOR RCS MEASUREMENTS OF A TARGET DOMINATED BY POINT SCATTERERS		5. TYPE OF REPORT & PERIOD COVERED MS THESIS 6. PERFORMING ORG. REPORT NUMBER
7. AUTHOR(s) BYRON M. WELSH 2nd Lt USAF		8. CONTRACT OR GRANT NUMBER(s)
9. PERFORMING ORGANIZATION NAME AND ADDRESS Air Force Institute of Technology(AFIT/EN) Wright-Patterson AFB, Ohio 45433		10. PROGRAM ELEMENT, PROJECT, TASK AREA & WORK UNIT NUMBERS
11. CONTROLLING OFFICE NAME AND ADDRESS Aeronautical Systems Division (ASD/ENAMA) Wright-Patterson AFB, Ohio 45433		12. REPORT DATE Dec. 1983 13. NUMBER OF PAGES 128
14. MONITORING AGENCY NAME & ADDRESS(if different from Controlling Office)		15. SECURITY CLASS. (of this report) UNCLASSIFIED 15a. DECLASSIFICATION/DOWNGRADING SCHEDULE

16. DISTRIBUTION STATEMENT (of this Report)

Approved for public release, distribution unlimited.

17. DISTRIBUTION STATEMENT (of the abstract entered in Block 20, if different from Report)

18. SUPPLEMENTARY NOTES

Approved for public release: IAW AFR 190-17

7 Feb 84

LYNN E. WOLAVER
Dean for Research and Professional Development
Air Force Institute of Technology (AIC)
Wright-Patterson AFB OH 45433

19. KEY WORDS (Continue on reverse side if necessary and identify by block number)

Radar Cross-Section
Radar Cross-Section Measurements
Minimum Range Criterion
Point Scattering

20. ABSTRACT (Continue on reverse side if necessary and identify by block number)

This thesis develops a minimum range criterion for radar cross-section measurements by neglecting the phase of the incident field at the target and considering only the amplitude distribution. In contrast to the traditional minimum range criterion, developed for a flat target characterized by specular reflection, the target examined in this thesis is characterized by a number of independent point scatterers

DD FORM 1 JAN 73 1473 EDITION OF 1 NOV 65 IS OBSOLETE

UNCLASSIFIED

SECURITY CLASSIFICATION OF THIS PAGE (When Data Entered)

located on the target surface. Instead of enforcing point by point accuracy, accuracy of the average target RCS is required, averaging over a number of measurements. The location of the point scatterers on the target are described probabilistically; the expected average measured RCS versus target range is calculated, and compared to results of a Monte-Carlo simulation. The traditional minimum range criterion is compared to the new minimum range criterion. The traditional minimum range criterion, based on phase uniformity across the target, requires minimum measurement ranges that are much larger than those ranges dictated by the new minimum range criterion for targets dominated by point scattering.